Resubmitted to the Journal of Sedimentary Research, April, 2005

DEPOSITIONAL TURBIDITY CURRENTS IN DIAPIRIC MINIBASINS ON THE CONTINENTAL SLOPE: FORMULATION AND THEORY

HORACIO TONIOLO[12], MICHAEL LAMB[13] AND GARY PARKER[1]

[1]*St. Anthony Falls Laboratory, University of Minnesota, Mississippi River at 3rd Ave. SE Minneapolis MN 55414 U.S.A.*
[2]*Now at University of Alaska Fairbanks, P.O. Box 755900, Fairbanks AK 99775-5900 U.S.A.*
[3]*Now at School of Oceanography, University of Washington, Seattle WA 98195-7940 U.S.A.*
e-mail: ffhat@uaf.edu, mike@ocean.washington.edu, parke002@tc.umn.edu

KEY WORDS: diapirs, minibasins, turbidity currents, ponding, water detrainment, hydraulic jump.

ABSTRACT: The northern continental slope of the Gulf of Mexico is riddled with numerous subsiding diapiric minibasins bounded by ridges, many but not all of which are connected by channels created by turbidity currents. The region is economically relevant in that many of these diapiric minibasins constitute focal points for the deposition of sand. Some of these sandy deposits in turn serve as excellent reservoirs for hydrocarbons. A better understanding of the "fill and spill" process by which minibasins fill with mud and sand as the intervening ridges are dissected by canyons may serve to aid in the location of such reservoirs. In the present paper a theory is developed to describe sediment deposition in minibasins. The theory relies on the hypotheses that the turbidity currents in question are sustained for at least about one hour. Two key and heretofore unrecognized aspects of the "fill and spill" process are revealed; a) the formation of an internal hydraulic jump as a turbidity current spills into a confined basin, and b) the detrainment of water across a settling interface forming at the top of the ponded turbidity current downstream of the hydraulic jump. It is shown that sufficiently strong detrainment can consume the flow, so that there is no outflow of either water or sediment even with continuous inflow. As the basin fills with sediment, however, overspill is eventually realized. The theory is developed into a numerical model, tested against experiments and applied at field scale in a companion paper.

INTRODUCTION

Turbidity currents on the continental slope have created a rich morphodynamic and stratigraphic record associated with erosion and deposition. The continental slope of the northern Gulf of Mexico offers a unique opportunity to study both of these simultaneously. A distinctive aspect of deep-water sedimentation in that region is the influence of fields of subsiding salt-withdrawal minibasins that have trapped thick sedimentary sections, some of which contain sand bodies with excellent hydrocarbon reservoir properties (Mahaffie 1994; Holman and Robertson 1994; Badalini et al. 2000). Regions of the northern continental slope of the Gulf of Mexico where minibasins abound are shown in Figures 1a and 1b (Pratson and Haxby 1997). The relief of each of these basins is on the order of hundreds of meters, and basin length ranges from kilometers to 10's of kilometers. Each basin is bounded by ridges that have been uplifted as a compensatory effect of basin subsidence. Many but not all of these minibasins are interconnected by drainage networks of turbidity current channels (e.g. Liu and Bryant 2000). The turbidity currents that created these channels have cut through the ridges to create canyons, and deposited sediment in the minibasins themselves, a process that has been documented by e.g. Beauboeuf and Friedman (2000) and Badalini et al. (2000).

Minibasins often contain layered deposits of turbidity currents in which either mud or sand dominate. Some of the sand bodies serve as good hydrocarbon reservoirs. In order for a turbidity current to deposit within a minibasin, however, it first must reach it. The initial stages by which this occurs can be envisioned in terms of a turbidity current that runs down the relatively steep slope of the updip rim of the minibasin, ponds within it, deposits sediment and eventually overflows. This process has been familiarly termed "fill and spill" (e.g. Winker 1996).

One approach to the study of the process of "fill and spill" is the analysis of the modern seafloor and the first few hundred meters below that level, using acoustic images of bathymetry and high-resolution seismic surveys and borehole drilling programs (e.g. Damuth et al. 1983; Malinverno et al. 1988; Bouma and Bryant 1994; Gardner et al. 1996; Winker 1996; Liu and Bryant 2000; Pirmez et al. 2000; Badalini et al. 2000 among many others). Such analyses have served to clarify many aspects of minibasins and the process by which they fill, several of which have been incorporated into the present work. In particular, they have revealed that the ultimate effect of "fill and spill" is to create a channel that cuts deeply though successive ridges and fills in successive basins, so connecting the basins and creating a channel with a relatively constant slope throughout. This evolution is summarized in Figure 2 (Beauboeuf and Friedman 2000). Note in Figure 2a, however, that the basin farthest downdip has not yet been filled to the point that an outlet channel has been excavated.

One limiting case for the process of "fill and spill" is the possibility that very large, sustained turbidity currents cascade from one basin to the next, simultaneously sculpting the channel of Figure 2 during each event. At the other end is the limiting case for which small, pulse-like events must substantially fill each minibasin before enough overflow occurs to initiate erosion through the ridge at the downdip end and start the process of filling of the next basin.

Field studies have supported argument toward the smaller end of the flows envisaged above (e.g. Badalini et al. 2000). Field studies in and of themselves may,

however, be insufficient to resolve these issues, which revolve about the dynamics of turbidity currents. Theory, experiment and numerical modeling offer alternate avenues with which to gain further insight in the process of "fill and spill." These avenues are explored here. They reveal a third possibility for the mechanism of "fill and spill:" namely, that sustained turbidity currents capable of eroding through the ridges may nevertheless be incapable of flowing out of a minibasin until the relief of the minibasin has been substantially reduced. Put in its simplest terms, the analysis presented here indicates that a sustained turbidity current flowing continuously into a minibasin may nevertheless produce no outflow whatsoever.

SUSTAINED VERSUS PULSE-LIKE TURBIDITY CURRENTS

Before proceeding, it is of value to clarify the term "sustained turbidity current," and indicate how such currents are generated and why they might be applicable to minibasin sedimentation. One limiting case of a turbidity current is a pulse-like event that consists of a head followed by very little body. There are ways, however, to generate turbidity currents that are sourced as sustained events, and in addition there are ways by which pulse-like events can evolve into more sustained events. The depositional mechanics of a sustained event are such that the role of the head is subsidiary to that of the body behind it.

One way in which sustained turbidity currents can be generated is through hyperpycnal river flows (Mulder and Syvitski 1995). These river flows are so heavily charged with sediment that they are heavier than sea water, and can thus plunge as they reach the ocean. The resulting turbidity current can be sustained for hours or days as long as the river flow remains hyperpycnal. The sediment concentrations in river water required to maintain hyperpycnal flow are, however, extremely high. For example, if the sea water is assumed to have a specific gravity of 1.026, the sediment in suspension in the river flow is assumed to have specific gravity of 2.65 and temperature differences between river water and sea water are neglected, the concentration of suspended sediment in the water column must exceed about 41,000 mg/l in order to maintain hyperpycnal flow. Mulder and Syvitski (1995) have documented the fact that hyperpycnal flows are not common in general. With the one exception of the Yellow River, China, under present-day conditions hyperpycnal flows are restricted to rivers which flow into the sea directly from active margins. Uplift along these margins drives an abundant sediment supply adjacent to the shelf. On passive margins such as the northern Gulf of Mexico in particular, present-day peak sediment concentrations of rivers are well under of 1/10 of the value necessary for hyperpycnal flows. For example, the maximum concentration listed for the Mississippi River at Tarbert Landing between October 1, 1974 and September 30, 1989 is 2910 mg/l (on March 6, 1984: see http://webserver.cr.usgs.gov/sediment/). Even at falling or low stand, it is difficult to construct a scenario under which such streams would have a sediment supply sufficient to create hyperpycnal flows.

This observation notwithstanding, there are four pieces of circumstantial evidence in support of sustained turbidity currents emanating from the northern margin of the Gulf of Mexico. The first of these pertains to the many moderately to highly sinuous leveed channels on the Mississippi Submarine Fan (Twichell et al. 1991) as well as within minibasins (Badalini et al. 2000; Beaubouef et al. 2003), and indeed on continental slopes

and submarine fans adjacent to passive margins all over the world (e.g. Pirmez 1994). The mechanism of meander formation, whether subaerial or subaqueous. requires a setup of a velocity and pressure field that requires a flow that has a spatial length of at least a few meander lengths (e.g. Ikeda et al. 1981; Imran et al. 1999). A pulse-like flow is not sufficient for this. The second of these pertains to the fact that these channels are typically bounded by substantial levees that in many cases extend for 100's of km. The implication is that the turbidity currents are self-channelizing. The only mechanisms that have been proposed for the process of self-chanelizing require sustained flows (Imran et al. 1998). The third of these pertains to Figures 2b and 2c describing the East Breaks minibasins. As shown in Figure 2b, turbidity currents have carved canyons over 200 m deep through the ridges created by compensational uplift between minibasins. Again, the only mechanisms that have been proposed for the excavation of deep submarine canyons involve sustained rather than pulse-like turbidity currents (Parker 1982; Fukushima et al. 1985; Parker et al. 1986). The fourth of these pertains to the delta-like structure observed in Basin IV of Figure 2a by Beaubouef et al. (2003). This structure closely parallels deltas built by sustained river flows. While these arguments do not prove conclusively that sustained turbidity currents have played a major role in the evolution of minibasins, they do suggest that in many cases they may have played a more important role than pulse-like events.

A number of mechanisms have been observed to be or proposed as generating agents for sustained turbidity currents. Surface wave action due to storms has been observed to trigger sustained turbidity currents (Inman et al. 1976; Puig et al. 2003). While surface waves are likely to be ineffective as means for generating turbidity currents on passive margins during the present high stand, they would have been much more effective during low stand, when river mouths were located much closer to the shelf-slope break. Breaking internal waves have been hypothesized to play a similar role in triggering sustained turbidity currents (e.g. Caccione et al. 2002). Retrogressive failure on e.g. a delta front provides another mechanism for the generation of sustained turbidity currents (e.g. Hay 1987). One mode of such retrogressive failure that is known to generate sustained turbidity currents is breaching (van den Berg et al. 2002; Mastbergen et al. 2003). Parsons and Garcia (2000) have proposed a double-diffusive mechanism for the generation of sustained turbidity currents from hypopycnal river flows.

The above mechanisms provide plausible means for generating sustained turbidity currents on passive margins at low stand. A turbidity current does not, however, need to initiate as a sustained current in order to evolve into one. Pantin (1979), Parker (1982), Fukushima et al. (1985) and Parker et al. (1986) have delineated a self-accelerative mechanism, termed "ignition" by Parker (1982), by which a relatively modest sustained turbidity can strengthen in the downstream direction by means of entrainment of sediment. Recently Pratson et al. (2000, 2001) have applied the model of Parker et al. (1986) to a turbidity current of discrete length, and shown how such a current can lengthen substantially as it self-accelerates. Put simply, under the right conditions a pulse-like turbidity current flowing over a surface covered with sediment available for entrainment can grow its way into a sustained turbidity current.

It is argued below that sustained turbidity currents likely play a major role in the process of sediment deposition within diapiric minibasins. It is useful to be more specific as to how long a current might be sustained. Although the issue is addressed in more

detail below, Lamb et al. (2004) provide evidence that in the case of the minibasins on the north slope of the Gulf of Mexico, a current that requires on the order of at least 30 minutes to pass by a given point should be sufficient to create the conditions described in this paper and its companion, Toniolo et al. (submitted).

INTERNAL HYDRAULIC JUMPS, WATER DETRAINMENT AND SETTLING INTERFACES

The research program that has led to the present work has its origins in the experiments of Hickson et al. (2000). They used high resolution bathymetric data of the Gulf of Mexico to derive a 'typical' intraslope basin topographic profile which was, in turn, used to construct a scale model of a) a single basin and b) two basins in succession. The experiments revealed two key features characteristic of sustained turbidity currents that are crucial to the present work; the internal hydraulic jump and the settling interface. These features have been confirmed by subsequent experimental work reported in Lamb et al. (2001), Violet et al. (2001), Toniolo (2002) and Lamb et al. (2004). Aspects of this work are summarized below. All the experiments in question were conducted in model minibasins with turbidity currents generated from dilute suspensions containing various combinations of a) grades of poorly sorted silica flour with nominal sizes of 110 μm, 45 μm and 20 μm, b) kaolinite clay, and c) glass beads (ballotini) with a nominal size near 45 μm.

Several aspects of internal hydraulic jumps and settling interfaces are described here without detailed justification. This justification is given later in the present paper and in the companion paper, Toniolo et al. (submitted). The issues are more easily discussed, however, after they have been introduced.

Hickson et al. (2000) found that as an experimental minibasin is filled by a continuous turbidity current, the downdip lip of the basin forces an internal hydraulic jump from swift flow upstream to placid, ponded flow downstream. A hydraulic jump is a type of shock associated with a sudden deceleration of flow (e.g. Henderson 1966). Its most familiar manifestation is in open channel flow. For example, swift, shallow flow on the steep spillway of a dam often undergoes a hydraulic jump as it flows into the deeper, more placid river downstream. A photograph of a hydraulic jump in open channel flow is presented in Figure 3a. Such hydraulic jumps are mediated by a dimensionless parameter known as the Froude number ***Fr***, which is defined as

$$\boldsymbol{Fr} = \frac{U}{\sqrt{gh}} \qquad (1a)$$

where U denotes depth-averaged flow velocity, h denotes flow depth and g denotes gravitational acceleration. Sufficiently swift, shallow flows have Froude numbers greater than unity and are called supercritical (or Froude-supercritical) flows. Sufficiently placid, deep flows have Froude numbers less than unity and are called subcritical (Froude-subcritical) flows. A steady supercritical open channel flow that empties into a deep, confined basin must undergo a hydraulic jump, as illustrated in Figure 3b. The deeper the basin the stronger will be the hydraulic jump. The flow downstream of a jump in a deep basin must consequently have a very low flow velocity, and an extremely low Froude number. Such placid, slow-moving flows are here called "ponded." As the flow approaches the downstream end of the basin, it must accelerate until it attains a critical Froude number of unity at the point of maximum elevation, i.e. the lip. Such points of

critical flow are called "controls" (e.g. Henderson 1966); the critical depth attained at the lip is denoted as h_e in Figure 3b.

It has long been recognized that dense bottom underflows driven by either salt, temperature differences or sediment can also undergo hydraulic jumps from swift to placid flow (e.g. Garcia 1993). Such jumps are called "internal hydraulic jumps" because they are bounded above by quiescent water that is free of the agent that drives the bottom underflow, e.g. sediment in the case of a turbidity current. Internal hydraulic jumps are mediated by the densimetric Froude number $\boldsymbol{Fr_d}$, which in the case of a turbidity current can be defined as

$$\boldsymbol{Fr_d} = \frac{U}{\sqrt{RCgh}} \qquad (1b)$$

where now h denotes the layer thickness of the turbidity current, U denotes layer-averaged flow velocity, C denotes layer-averaged volume sediment concentration and R denotes the submerged specific gravity of the sediment in suspension (~ 1.65 for many natural sediments. Again, a critical value of $\boldsymbol{Fr_d}$ near unity divides subcritical and supercritical flows.

Garcia and Parker (1989) and Garcia (1993) performed experiments on continuous depositional turbidity currents undergoing internal hydraulic jumps mediated by a drop in slope from a finite, constant value of 0.08 to a horizontal bed. The turbidity current was vented out of the tank via a submerged overfall, which forced a critical densimetric Froude number of unity there. This case is illustrated in Figure 4a. The incoming flow is supercritical, a condition that allows it to vigorously entrain ambient water from above across a diffuse, turbulent interface. The drop in slope causes a hydraulic jump to a subcritical flow which still has a somewhat turbulent interface, but which entrains little ambient water. The flow first decelerates down the tank as sediment deposits out, but then reaccelerates to a critical densimetric Froude number of unity at the submerged outfall. The nature of the deposit created by such a flow is illustrated in Figure 4a. Note that the deposit becomes thinner downstream.

Hickson et al. (2000) and Lamb et al. (2004), however, found that the hydraulic jump is manifested somewhat differently in the presence of a high barrier at the downstream end of a model minibasin. In order to illustrate this in the simplest way, the barrier is schematized as a vertical wall in Figure 4b. Sustained flow is introduced into the basin defined by the upstream slope and the downstream wall. The barrier forces a sharp hydraulic jump, downstream of which a muddy pond forms. If the barrier is of sufficient height the flow in the muddy pond becomes thick and slow-moving, so that the densimetric Froude number is much less than unity. Under such conditions a distinct, relatively sharp interface forms between the muddy pond and the clear water above. An example of such a sharp interface in an experimental minibasin is shown in Figure 4c. As long as the sediment in the turbidity current is uniform, deposit thickness downstream of the hydraulic jump is approximately constant in the streamwise direction, as shown in Figure 4b. This result, which is a direct consequence of ponding, is demonstrated theoretically below and experimentally in the companion paper, Toniolo et al. (submitted).

The interface in question is a settling interface. Consider a graduated cylinder with cross-sectional area A containing water in which a small amount of sediment has been mixed uniformly in the vertical with volume concentration C. For the sake of

argument the sediment is assumed to have a uniform size. If the agitation is terminated and the sediment is allowed to settle, it will form a distinct settling interface that migrates downward at the fall velocity v_s of the sediment. This interface converts dirty water into clear water, as illustrated in Figure 5. The upward discharge across the interface from the turbid zone to the clear zone is here defined as the detrainment discharge Q_d, where

$$Q_d = Av_s \quad (2)$$

The sediment concentration in the water column remains constant over time with the value C, because as the sediment settles out on the bed at rate v_sC (so acting to reduce the concentration) the vertical extent of the zone containing sediment decreases (so acting to increase concentration) at the same rate. The two effects exactly balance each other.

The settling interface shown in the ponded zone of the experimental minibasin shown in Figure 4c is similar to that in Figure 5, but differs in an important way. Its vertical position does not lower in time, because the water discharge lost to detrainment is replaced by the water in the turbidity current flowing in from upstream. If the slow, gradual accumulation of sediment on the bed by deposition from the dilute suspension is neglected for the sake of argument, a perfectly stable settling interface can be created in a minibasin when the rate of detrainment of water across the interface downstream of the hydraulic jump perfectly balances the difference between the rate of inflow of water from upstream and the rate of outflow across the downstream lip of the minibasin. That such a balance can bed reached is demonstrated theoretically in the present paper and numerically and experimentally in the companion paper, Toniolo et al. (submitted). The gradual accumulation of sediment implies, however that the interface should slowly rise in time as the basin fills.

A limiting case of the above argument is one for which detrainment is able to perfectly balance the inflow, in which case there is no flow spilling out of the basin, all of the water is lost to detrainment and all of the sediment is captured in the basin. Again, this is demonstrated theoretically in the present paper and numerically and experimentally in the companion paper, Toniolo et al. (submitted).

The above observations suggest the flow pattern of a continuous turbidity current in a deep minibasin described in Figure 6a. The configuration of Figure 6a schematizes what was actually used for the experiments of Hickson et al. (2000), Lamb et al. (2001) and Lamb et al. (2004). Figure 6a is entirely analogous to the open channel flow in a confined basin described in Figure 3b, but with the following differences. In the case of a turbidity current ambient water can be entrained into the zones of supercritical flow, and water can be detrained across the settling interface of the ponded zone. If the flow upstream of the hydraulic jump has sufficient discharge to overcome the water detrainment in the ponded zone, the interface in the ponded zone will lie above the downstream lip (the solid line in the ponded zone), and there will be outflow of current and sediment from the basin. If on the other hand all the forward discharge of the turbidity current is consumed by detrainment in the ponded zone, the interface there will lie below the downstream lip (dashed line in the ponded zone) and neither current nor sediment will spill out of the basin.

Figure 6b describes the process by which initial overspill from the lip of an upstream minibasin leads to the setup of quasi-steady flow in the basin downstream. At time t_1 a ponded turbidity current has not yet overflowed the lip of the upstream basin. At time t_2 overflow has commenced. A critical densimetric Froude number has been

established at the overflow lip of the upstream basin, and a turbidity current with a distinct head has penetrated into the downstream basin. By time t_3 this head has reflected off the downstream barrier of the downstream minibasin, and is migrating upstream as a bore. By time t_4 the bore has stabilized as an internal hydraulic jump, and quasi-steady flow has been established. In the example of Figure 6b, the interface of the muddy pond lies below the downstream lip of the downstream basin, but as shown in Figure 6a, it can also lie above this point depending on the balance between inflow and detrainment. The process of setup is described in more detail in Lamb et al. (2004).

An internal hydraulic jump did not appear in several of the experiments of Lamb et al. (2004). This is because the elevation of the lip at the downstream end of the minibasin was sufficiently high to cause the muddy pond to back up and drown the incoming flow from the bottom gate at the upstream end of the basin. In such a case the incoming flow formed a drowned plume that emanated from the bottom gate as a Froude-subcritical flow.

Fluid detrainment from a sediment-laden flow has been described previously by Sparks et al. (1993). They consider the cases of a) a turbidity current containing water that is lighter than the ambient water above due to differences in temperature or dissolved salt concentration and b) a subaerial pyroclastic flow containing volcanic ash and air that is substantially hotter, and thus lighter than the ambient air above. The runout distance of the turbidity current or pyroclastic flow is limited by the tendency of the fluid in the flow (water or air) to detrain upward due to the density difference. Once enough sediment has settled out so that the flow is lighter than the ambient fluid, the flow will be wafted upward, so limiting runout. The detrainment described here is similar to that of Sparks et al. (1993), but is different in that it is entirely mediated by the tendency of sediment to fall out, and does not require any density difference between the water in the turbidity current and that in the ambient water above.

Before proceeding, it is useful to ask whether or not the above concepts have applicability to the field setting.

PONDING AND DETRAINMENT AT FIELD SCALE

Consider for the sake of argument a turbidity current containing uniform 100 μm material flowing into a basin with a top area of 10 km^2, a fairly typical size for the northern continental slope of the Gulf of Mexico. Using the relation for fall velocity of Dietrich (1982) it is found that v_s = 7.48 mm/s. The potential detrainment discharge Q_{pd} realized if detrainment occurs across a surface equal to the top area of the minibasin is found from Equation 2 to be 748,000 m^3/s. Hill (1998) reports that fine-grained marine sediments tend to naturally flocculate to a fall velocity of 1 mm/s. If the turbidity current were composed solely of such material, the potential detrainment discharge would be 100,000 m^3/s. For reference, the mean discharge of the Mississippi River is on the order of 17,000 m^3/s, and the peak discharge of the flood of 1927 has been estimated to be in the range 70,000 – 80,000 m^3/s (e.g. Barry 1997). The implication is that the potential for detrainment to limit overspill from basin to basin is enormous at field scale.

Neither ponding nor detrainment have been observed for the case of natural oceanic turbidity currents, and as a result they are likely to be unfamiliar phenomena to many submarine geologists. Fortunately, an excellent example of both is provided by the case of the disposal of mine tailings into Lake Superior by the Reserve Mining Company

during the period 1955-1974 (e.g. Normark and Dickson 1976). Sand- and silt-sized tailings were disposed as slurry into Lake Superior at Silver Bay. The coarser sediment deposited to form a delta; the finer sediment continued into deep water as a quasi-continuous turbidity current. Immediately offshore of Silver Bay the bathymetry describes a localized, confined basin with a maximum depth of about 280 m (Figure 7a). Both turbidity current ponding and water detrainment are vividly illustrated by measurements taken during a strike from July 31 to August 27, 1972 (Normark, personal communication). During the strike the mine was forced to cease tailings disposal.

Acoustic transmissivity measurements were used to track patterns of turbidity in the basin as the strike progressed. These measurements are shown in Figures 7b-7f for the dates July 31, August 2, August 8, August 19 and August 25, all in 1972. A zone of ponded turbid water with a clear upper interface is apparent in Figure 7b, shortly after the beginning of the strike. The ponded zone is piled against the northern side of the basin wall, probably due to wind-driven internal seiching. With no inflow of sediment, however, the interface is seen to gradually move downward in Figures 7c-7e as the sediment settles out, detraining turbid water in the process. By August 25 the interface has vanished completely, implying that all the sediment has settled out and all the turbid water has clarified.

Comparing Figures 7d and 7f, it can be seen that the settling interface migrated downward about 40 m in about 16 days. This corresponds to a settling velocity of 0.029 mm/s. The quartz grain size with this fall velocity in clear water at 20° C is 18 μm according to the relation of Dietrich (1982). This size is consistent with the finer sizes of the tailings disposed by the mine. Although seiching is present in Figures 7b-7f, it cannot be expected to help maintain sediment in suspension unless it contributes to a bottom boundary layer that accomplishes resuspension of settled sediment.

FORMULATION OF THE THEORY

This paper focuses on the study of minibasin deposition in a highly simplified configuration. A slot-like minibasin is assumed to be much longer than it is wide. The turbidity current flowing into it is continuous and carries a dilute suspension of sediment of uniform size with a fall velocity v_s. The minibasin is assumed to have sufficient relief to cause the inflowing turbidity current to undergo a hydraulic jump, so creating a muddy pond with a very low densimetric Froude number containing a dilute suspension of very slowly moving water and sediment. The interface between the muddy pond and the clear water above defines a settling interface. This interface may be above the elevation of the lip at the downstream end of the pond, in which case the turbid water overflows the basin, or below it, in which case there is no overflow. In the latter case all the sediment is lost to bed deposition and all the inflowing water is lost to detrainment across the settling interface. This geometry is illustrated in Figure 6a. The above simplifications serves to clearly define the roles of the internal hydraulic jump and water detrainment in mediating the process of minibasin deposition. They can be relaxed at a later date.

Now let t denote time, x denote a bed-attached streamwise coordinate, y define a coordinate directed upward normal from the bed and assumed quasi-vertical, h denote the depth of the muddy pond, and (u, v) denote the local flow velocities in the (x,y) directions (averaged over any turbulence in the ponded zone).

The flow in the ponded zone is assumed to be slow, and any turbulence within it is assumed to be too weak to entrain a) water across the settling interface, and b) sediment from the bed. In this case the equations of water mass balance, sediment mass balance and momentum balance can be written in the respective forms

$$\frac{\partial u}{\partial x}+\frac{\partial v}{\partial y}=0$$

$$\frac{\partial c}{\partial t}+\frac{\partial uc}{\partial x}+\frac{\partial vc}{\partial y}-v_s\frac{\partial c}{\partial y}=0 \qquad \text{(3a,b,c)}$$

$$\frac{\partial u}{\partial t}+\frac{\partial u^2}{\partial x}+\frac{\partial uv}{\partial y}=-Rg\frac{\partial}{\partial x}\int_y^h c\,dy+RgcS+\frac{1}{\rho}\frac{\partial \tau}{\partial y}$$

where R denotes the submerged specific gravity of the sediment (near 1.65 for many natural sediments), ρ denotes the density of clear water, c denotes volume concentration of sediment, here assumed to be small, τ denotes the bed shear stress and bed slope S is given as

$$S=-\frac{\partial \eta}{\partial x} \qquad (4)$$

where η denotes the bed elevation from an arbitrary level (e.g. Parker et al. 1986). The above relations employ the slender flow approximations, according to which the horizontal extent of the body of ponded turbid water must be much larger than the depth of the ponded zone.

Equations 3a-3c are subject to boundary conditions. The bed is assumed to be impermeable, so that

$$u\big|_{y=0}=v\big|_{y=0}=0 \qquad (5)$$

The interface is described by a variant of the kinematic boundary condition taking the form

$$\frac{\partial h}{\partial t} + u\big|_{y=h}\frac{\partial h}{\partial x} = v\big|_{y=h} - v_s \qquad (6a)$$

In the simple settling tube of Figure 5, for example, Equation 6a reduces to

$$\frac{\partial h}{\partial t} = -v_s \qquad (6b)$$

so that in the absence of replenishing turbid flow the interface is advected downward with the fall velocity of the sediment.

Equations 3a-3c are now integrated from the bed to the settling interface of the minibasin. It is assumed that sediment is carried into the basin by a Froude-supercritical turbidity current, and that an internal hydraulic jump has acted to mix the sediment uniformly in the vertical in the muddy pond downstream. The fact that an internal hydraulic jump to a strongly ponded flow created by a downstream barrier can indeed create a suspension in which sediment of uniform size is mixed approximately uniformly in the vertical is demonstrated experimentally in the companion paper, Toniolo et al. (submitted).

Since passive settling in the absence of resuspension must occur in a strongly ponded zone due to the very slow flow velocities, as one layer of sediment in the water column settles it is replaced from above by another layer with the same concentration. Thus concentration c can be taken as equal to a constant C in y between $y = 0$ and $y = h$, i.e.

$$c(x,y,t) = C(x,t) \qquad (7)$$

Integrating Equation 3a from 0 to h under the conditions of Equations 5 and 6a, it is found that

$$\frac{\partial h}{\partial t} + \frac{\partial Uh}{\partial x} = -v_s \qquad (8)$$

where

$$U = \frac{1}{h}\int_0^h u\,dy \qquad (9)$$

denotes the layer-averaged streamwise flow velocity in the ponded zone. Note that the term $-v_s$ on the right-hand side of Equation 8 quantifies the rate of loss of water across the settling interface.

A similar integration of Equation 3b with the aid of Equations 5, 6a and 7 yields the following relation for the conservation of suspended sediment;

$$\frac{\partial Ch}{\partial t} + \frac{\partial UCh}{\partial x} = -v_s C \qquad (10)$$

Note that in accordance with the assumptions outlined above, this relation does not allow for re-entrainment of sediment lost from the suspension by settling. The corresponding Exner equation of bed sediment conservation takes the form

$$(1-\lambda_p)\frac{\partial \eta}{\partial t} = v_s C \qquad (11)$$

where λ_p is the sediment porosity of the deposit in the minibasin. Finally, after some work it is found that the integral of Equation 3c is

$$\frac{\partial Uh}{\partial t}+\frac{\partial U^2 h}{\partial x}+Uv_s=-\frac{1}{2}Rg\frac{\partial Ch^2}{\partial x}+RgChS-(C_{f0}+C_{fI})U^2 \qquad (12)$$

In deriving Equation 12, it has been assumed that local velocity u can be approximated with its layer-averaged value U from $y = 0$ to $y = h$ in evaluating the last two terms on the left-hand side. In addition, the shear stresses at the bed and settling interface have been related to the square of the flow velocity by means of the parameters C_{f0} and C_{fI} denoting bed and interfacial friction coefficients.

ANALYTICAL SOLUTION

Relations for concentration C and condition for overflow. Cross-eliminating between Equations 8 and 10, it is quickly found that the relation governing the concentration C in the basin is a simple kinematic wave equation;

$$\frac{\partial C}{\partial t}+U\frac{\partial C}{\partial x}=0 \qquad (13a)$$

That is, any given concentration C at the upstream end of the basin (i.e. just beyond the hydraulic jump) is advected without change at velocity U down the basin. In the case of steady flow, (13a) reduces to the condition

$$C=\begin{cases} const \quad , & 0\le y\le h \\ 0 \quad , & y>h \end{cases} \qquad (13b)$$

The above relation is of some significance. If the water and sediment input to the basin is steady, the flow in the ponded zone can be treated as quasi-steady, with a constant sediment concentration throughout its length. The flow is not truly steady, because sediment deposition builds the bed upward in time, but in the case of a dilute turbidity current this process is very slow compared to the setup time for the hydraulic jump and ponding. It is seen from Equations 11 and 13b that for quasi-steady conditions the bed in the ponded zone builds up at the same speed everywhere in the ponded zone, implying a deposit of uniform thickness in the streamwise direction.

The condition of constant concentration may not be satisfied in a short zone near the downstream overflow lip of Figure 6. The flow must accelerate in this region to overspill, in which case the condition of vanishing entrainment from the bed may not be satisfied locally.

Whether or not the flow spills out of the basin is determined from Equation 8. The forward volume flow discharge per unit width is denoted as q, where

$$q=Uh \qquad (14)$$

For a quasi-steady flow Equation 8 may be integrated to yield

$$q=q_o-v_s x \qquad (15)$$

where q_o denotes the value of q just beyond the hydraulic jump. Let L denote the length of the ponded zone from the hydraulic jump to the overflow point. Overflow occurs only if

$$q_o-v_s L>0 \qquad (16)$$

Condition 16 deserves some elaboration. Let B denote the width of the basin, Δh denote maximum basin relief and L_b denote its length. The potential detrainment discharge from the basin is given from Equation 2 as $Q_{pd} = BL_b v_s$. The inflow discharge is given as $Q_o = Bq_o$. The length L from the hydraulic jump to the downstream end of the

basin is in general less than L_b. It can be expected to decrease with increasing inflow discharge Q_o as the flow forces the hydraulic jump downstream, and increase with increasing relief Δh as the ponded flow backs up behind the barrier. According to Condition 16, if the actual detrainment discharge $Q_d = BLv_s$ is greater than the inflow discharge, then all of the forward discharge in the muddy pond is consumed by detrainment. In this case all the sediment deposits in the basin, and there is no overflow.

If such a flow were continued long enough, or a sufficient number of such flow events were repeated, the basin would gradually fill with sediment, so reducing the relief Δh. This reduction would in turn lower the value of L to the point that the detrainment discharge becomes less than the inflow discharge, eventually resulting in overflow of the turbidity current.

Shape of the interface. Equation 12 can be manipulated with the aid of Equations 4 and 8 to yield the following relation;

$$\frac{\partial U}{\partial t} + U\frac{\partial U}{\partial x} = -RgC\left(\frac{\partial \xi}{\partial x} + \frac{1}{2}\frac{h}{C}\frac{\partial C}{\partial x}\right) - (C_{f0} + C_{fl})\frac{U^2}{h} = 0 \qquad (17)$$

where

$$\xi = \eta + h \qquad (18)$$

denotes the elevation of the settling interface. If the flow is sufficiently slow the quadratic drag terms in Equation 17 may be neglected. (This assumption may break down right near the overflow point, where the flow re-accelerates.) In the case of steady flow, then, Equation 17 reduces with the aid of Equation 13b to

$$\frac{d}{dx}\left(\frac{1}{2}U^2 + RgC\xi\right) = 0 \qquad (19a)$$

or thus

$$\frac{1}{2}U^2 + RgC\xi = const \qquad (19b)$$

i.e. a Bernoulli equation for the muddy underflow.

Wherever the basin is sufficiently deep, the first term on the left-hand side of Equation 19b will be small compared to the second term on the left-hand side, resulting in the condition of an interfacial elevation ξ that is constant everywhere in space, i.e.

$$\xi = const \qquad (19c)$$

This condition can be expected to be satisfied everywhere except in the vicinity of the overflow lip in the case of sufficient ponding.

The turbidity current overflows the basin in the event that Condition 16 is satisfied. Let U_e denote the flow velocity, h_e denote the flow thickness, η_e denote the bed elevation and ξ_e denote the interface elevation at the overflow point. At that point the densimetric Froude number must be equal to unity, i.e.

$$\frac{U_e^2}{RgCh_e} = \frac{q_e^2}{RgCh_e^3} = 1 \qquad (20)$$

where $q_e = U_e h_e$ denotes the overflow discharge per unit width. (In point of fact the concentration of sediment at the overflow point may be somewhat elevated due to the inhibition of settling, or even the onset of sediment entrainment by high velocity just upstream.) Let ξ_p denote the constant elevation of the interface in the ponded zone of the

basin, i.e. well upstream of the overflow point, within which the term *1/2* U^2 can be neglected compared to $RgC\xi_p$ in Equation (19b) . It then follows from Equation 19b that

$$RgC(\xi_p - \xi_e) = \frac{1}{2}U_e^2 \qquad (21a)$$

Between Equations 20 and 21a, then,

$$\xi_p = \xi_e + \frac{1}{2}h_e = \eta_e + \frac{3}{2}h_e = \eta_e + \frac{3}{2}\left(\frac{q_e^2}{RgC}\right)^{1/3} \qquad (21b)$$

The above condition allows for computation of the height of the interface at the point of basin overflow as a function of lip elevation η_e, outflow discharge per unit width q_e and concentration C.

Sediment deposition within the basin. According to Equation 13b the sediment concentration C is not only constant in the vertical, but also constant in the streamwise direction, at least from the hydraulic jump to a point not far upstream of the downstream overflow lip where the flow sufficiently re-accelerates to cause sediment entrainment. In between these two zones, the rate of sediment deposition on the bed is given as v_sC, implying that the deposit should consist of a pure drape of thickness that is constant in the streamwise direction. Solving Equation 11 for a quasi-steady flow, deposit thickness is seen to vary in time as

$$\eta = \eta_I(x) + \frac{v_s C}{(1-\lambda_p)}t \qquad (22)$$

where $\eta_I(x)$ denotes the initial profile of the bed.

DISCUSSION

The above model hinges on three key assumptions. These are a) a downstream barrier can force a relatively sharp hydraulic jump to strongly ponded flow with a relatively sharp settling interface, b) the hydraulic jump can mix the suspended sediment approximately uniformly in the vertical up to the interface, and c) water can detrain across the muddy interface in the ponded zone. The justification of these assumptions is presented in the companion paper, Toniolo et al. (submitted).

The solution for the flow obtained in the previous section, applied to the case of a basin with a horizontal floor, a vertical downstream barrier with no overflow, is illustrated in Figure 8. Within the ponded zone layer-averaged suspended sediment concentration C is constant in x in accordance with Equation 13b. The elevation of the interface ξ, and thus the flow depth h for the geometry of Figure 8, are constant in x in accordance with Equation 19c. The condition of constant h combined with Equations 14 and 15 and the geometry of Figure 8 yield a flow velocity that declines linearly in x to 0 at the barrier;

$$U = \frac{q_o}{h}\left(1 - \frac{x}{L}\right) \quad , \quad v_s L = q_o \qquad (23a,b)$$

The above model assumes continuous rather than pulse-like inflow into the basin. This implies a turbidity current that is sustained for enough time for the hydraulic jump and ponded flow to set up. The process of ignition described by Parker et al. (1986) (see also Pantin 1979; Parker 1982 and Pratson et al. 2000, 2001) provides a mechanism by which pulse-like flows generated near the shelf-slope break can grow into quasi-

continuous events farther downstream. Even if each flow is continuous, the actual deposit realized in the basin is a result of the stacking of deposits from each flow.

In order for the quasi-continuous flow to set up, the head of the current must reach the downstream end of the basin, reflect back as an upstream-migrating bore and then stabilize as an internal hydraulic jump, as shown in Figure 6b. Lamb et al. (2004) have estimated that the current must be sustained for a time that is at least on the order of 30 seconds beyond the initial reflection of the bore for this to occur at the scale of the laboratory experiments described therein (which is similar to those described in the companion paper, Toniolo et al., submitted). The corresponding time scale they obtained based on an estimate of field-scale flows in minibasins in the Gulf of Mexico is 30 minutes.

For the sake of reference the relation of Lamb et al. (2004) for this time scale is reproduced here. The flow illustrated in Figure 6b is considered. The minimum time for the setup of a quasi-steady ponded flow is the time from when the head of the turbidity current reaches the downstream end of the basin to when the resulting reflected bore reaches a point near the upstream end of the basin where it stabilizes as a hydraulic jump. This time is denoted as T_b. The distance from the position of the hydraulic jump to the downstream end of the basin can be estimated as the basin length L_b. Denoting the sediment concentration of the turbidity current as C and the elevation difference from the interface of the inflowing turbidity current before reflection to the upper interface of the bore after reflection as Δh, the time T_b is given as

$$T_b \approx \frac{L_b}{\sqrt{RgC\Delta h}} \qquad (24)$$

For example, if L_b = 10,000 m, Δh = 100 m, R = 1.65 and C = 0.01, the estimate of T_b for the minimum time to set up quasi-steady flow with a hydraulic jump is found from Equation 24 to be about 41 minutes.

The assumption of a vertical profile of suspended sediment concentration of Equation 13 that is constant up to the interface may give the impression that flow stratification effects have been neglected. This is by no means the case. The actual concentration profile, along with the step approximation of Equation 13 are illustrated in Figure 9. The step approximation provides an extreme case of stratification, according to which stratification at the interface is so strong that turbulence is strongly damped there and a very sharp interface is manifested. This sharp interface is illustrated in Figure 4c. It is also seen in another type of highly stratified environment, i.e. the atmospheric inversion. In such cases a sharp density interface often bounds the clear air above from e.g. pollution-laden city air.

It might be argued that the interface shown in Figure 4b ought to decline in the streamwise direction as sediment settles out. Such behavior would be expected for a slow-moving turbidity current flowing over an unbounded domain. The wall at the downstream end of Figure 4b, however, radically changes the flow configuration. The flow velocity must drop to zero at the downstream wall. As sediment settles out and the interface starts to migrate downward, very slow flow from behind replenishes it and re-establishes the original position of the interface. Were the interface to decline in the streamwise direction, this decline would set up a pressure difference that would act to restore the nearly horizontal settling interface, as illustrated in Figure 10. The slower the

flow is in the ponded region, the less able is flow momentum to counter this restoring pressure force.

Application of the model presented in the previous section to either experimental or field flows is limited by the fact that it does not predict the position of the hydraulic jump, and thus the length *L* of the ponded zone. A full numerical model is needed for this. Such a model is pursued in the companion paper, Toniolo et al. (submitted).

The analysis of this paper and the experiments of the companion paper, Toniolo et al. (submitted) are based on a model minibasin of constant width, receiving inflow across the entire width. In such a case the degree of ponding is controlled largely by basin relief. In the field, however, the initial overspill into a minibasin can be expected to occur over a much narrower zone corresponding to a saddle in the upstream lip (which would later evolve into a canyon through incision). As a result the flow must expand laterally as it enters the minibasin. As a result the degree of ponding in the field can be expected to be stronger than that in the laboratory configuration described here.

It should be noted that the theory places no restriction on the size or settling velocity v_s of the sediment in the turbidity current. As long as the assumptions of the theory are met, the sediment may be in the sand, silt or clay sizes. The finer the sediment for the same size basin, the lower is the potential detrainment discharge, and so the more likely it is that overspill from a sustained event will be realized. The sedimentation rate in the ponded zone is determined solely by the concentration C and the fall velocity v_s, and therefore will be only as rapid as the fall velocity permits.

Turbidity currents can be expected to contain multiple grain sizes. It can be speculated that in this case the basin would contain multiple settling interfaces, with the interface corresponding to a coarser size being below one corresponding to a finer size. This is schematized in Figure 11 for a case in which there are a discrete number of sediment sizes. The condition for maximum "net to gross" (maximum sand content in the deposit) would then be one for which the interface for silt sizes is above the downstream lip of the basin, but the one for sand sizes is below it. A complete theory for multiple grain sizes, however, remains to be worked out.

It is unlikely that the conditions for a hydraulic jump to ponded flow are maintained indefinitely through geomorphic time. Increasing overflow across the downstream lip of a basin can ultimately lead to incision into the ridge bounding that basin and one immediately downstream. This incision can progress to the point that a smooth long profile is established through both basins and the ridge in between. The barrier causing the hydraulic jump and ponding will then have cut through. As seen in Figures 2b and 2c, as much as 200 m of incision into the ridges is required to establish this smooth profile. Incision is not described either in this paper or its companion, Toniolo et al. (submitted), which focus on the initial process of spill.

CONCLUSION

A simplified model of ponded turbidity currents containing sediment of uniform size predicts that the concentration *C* in the ponded zone should be constant in the streamwise direction. As a result, the deposit should be of spatially uniform thickness. The assumptions leading to this conclusion may break down in a small region near the overflow point where the ponded current re-accelerates.

The outflow discharge overflowing the lip at the downstream end of the minibasin is predicted to be less than the inflow discharge due to the effect of water detrainment. If the ponded zone is sufficiently long, there may be no outflow of either water or sediment across the lip. Estimates of the effect of detrainment at field scale suggest extremely large potential detrainment discharges, indicating that even with inflow from a succession of large, quasi-continuous events, there may be relatively little outflow from a minibasin until its relief has been reduced substantially.

The above results hinge on several key assumptions. These assumptions are justified, and the analysis is pursued quantitatively in the companion paper, Toniolo et al. (submitted).

ACKNOWLEDGMENTS

This research was supported by the Office of Naval Research STRATAFORM Program and the St. Anthony Falls Oil Consortium. The authors thank William Normark for providing data on ponded turbidity currents in Lake Superior.

NOTATIONS

A	$= LB$; top area of the ponded zone of a turbidity current
B	width of the basin
c	volume concentration in the turbidity current
C	layer-averaged volume concentration in the turbidity current
C_{f0}	bed friction coefficient
C_{fl}	interfacial friction coefficient
$\boldsymbol{Fr}$	Froude number of open-channel flow
$\boldsymbol{Fr_d}$	densimetric Froude number
g	acceleration of gravity
h	turbidity current thickness
L	length of the ponded zone of the turbidity current
L_b	length of the basin
Q	flow discharge of the turbidity current
Q_o	inflow discharge just before the hydraulic jump
Q_d	detrainment discharge of a ponded turbidity current
q	flow discharge per unit width
q_o	inflow discharge per unit width just before the hydraulic jump
q_e	value of flow discharge per unit width at the downstream overflow lip
R	$= (\rho_s/\rho - 1)$, submerged specific gravity of sediment
S	bed slope
T_b	estimate of the setup time for a quasi-steady flow in a minibasin
t	time
x, y	streamwise and upward normal directions
u, v	flow velocity in the ponded turbidity current in the x, y directions
U	layer-averaged streamwise velocity of the ponded turbidity current
U_e	value of U at the downstream overflow lip.
v_s	fall velocity of the sediment in the turbidity current
λ_p	sediment porosity

Δh	elevation difference between the upper interface of a bore reflecting from the downstream end of a minibasin and the upper interface of the incoming turbidity current before it reflects
η	bed elevation
η_e	bed elevation at the downstream overflow lip
ξ	elevation of the interface between muddy ponded water and clear water above
ξ_e	interface elevation at the downstream overflow lip.
ρ	density of water
ρ_s	density of sediment
τ	shear stress

REFERENCES

BADALINI, G., KNELLER, B. AND WINKER, C.D., 2000, Architecture and processes in the late Pleistocene Brazos-Trinity Turbidite System, Gulf of Mexico Continental Slope: *Proceedings*, GCSSEPM Foundation 20th Annual Research Conference, Deep-Water Reservoirs of the World, p. 16-34.

BARRY, J. M., 1997, *Rising Tide:* Simon and Schuster, New York, 574 p.

BEAUBOUEF, R.T., AND FRIEDMAN, S.J., 2000, High resolution seismic/sequence stratigraphic framework for the evolution of Pleistocene intra slope basins, western Gulf of Mexico: depositional models and reservoir analogs: *GCSSEPM Foundation 20th Annual Research Conference*, Deep-Water Reservoirs of the World, Dec. 3-6, 40-60.

BEAUBOUEF, R.T., VAN WAGONER, J.C., AND ADAIR, N. L., 2003, Ultra-high resolution 3-D characterization of deep-water deposits- II: Insights into the evolution of a submarine fan and Comparisons with River Deltas: *AAPG Annual Convention*, Extended Abstracts, May 11-14, Salt Lake.City, Utah, 9p.

VAN DEN BERG, J.H., VAN GELDER, A., AND MASTBERGEN, D.R., 2002. The importance of breaching as a mechanism of subaqueous slope failure in fine sand: *Sedimentology*, 49,(1), 81-95.

BOUMA, A.H., AND BRYANT, W.R., 1994, Physiographic features on the northern Gulf of Mexico continental slope: *Geo-Marine Letters,* v. 10, p. 182-199.

CACCHIONE, D.A, PRATSON, L.F., AND OGSTON, A.S., 2002, The shaping of continental slopes by internal tides: *Science*, 296(5568), 724-727.

DAMUTH, J.E., KOLLA, V., FLOOD, R.D., KOWSMANN, R.O., MOONTEIRO, M.C., GORINI, M.A., PALMA, J.J.C., AND BELDERSON, R.H., 1983, Distributary channel meandering and bifurcation patterns on Amazon deep-sea fan as revealed by long-range side-scan sonar (GLORIA): *Geology*, v. 11, p. 94-98.

DIETRICH, E.W., 1982, Settling velocities of natural particles: *Water Resources Research*, 18 (6), p. 1626 – 1682.

FUKUSHIMA, Y., PARKER, G. AND PANTIN, H., 1985, Prediction of igniting turbidity currents in Scripps Submarine Canyon: *Marine Geology*, 67, 55-81.

GARCIA, M.H., 1993, Hydraulic jumps in sediment-driven bottom currents: *Journal of Hydraulic Engineerin*g, ASCE, 119(10), p. 1-24.

GARCIA, M.H., AND PARKER, G., 1989, Experiments on hydraulic jumps in turbidity currents near a canyon-fan transition: *Science*, 245, p. 393-396.

GARDNER, J.V., FIELD, M.E., AND TWICHELL, D.C., 1996, Geology of the United States' Seafloor: The view from GLORIA: Cambridge University Press, Cambridge, 364 p.

HAY, A. E., 1987, Turbidity currents and submarine channel formation in Rupert Inlet, British Columbia. II. The roles of continuous and surge-type flow: *Journal of Geophysical Research*, 92, 2883-2900.

HENDERSON, M., 1966, Open Channel Flow: Prentice-Hall, 522 p.

HICKSON, T., SHEETS, B., AND MARR J., 2000, Filling of intraslope basins by turbidity currents: results from experimental simulations: *Abstracts*, American Association of Petroleum Geologists, 2000 Annual Convention, April 16-19.

HILL, P. S., 1998, Controls on floc size in the coastal ocean: *Oceanography*, 11(2), 13-18.

HOLMAN, W.E., AND ROBERTSON, S.S., 1994, Field development, depositional model, and production performance of the tubiditic "J" sands at Prospect Bullwinkle, Green Canyon 65 fields, outer-shelf Gulf of Mexico. In: Weimer, P., Bouma, A. H. and Perkins, B. F. eds., Submarine fans and turbidite systems – sequence stratigraphy, reservoir architecture, and production characteristics: Gulf Coast Section, Society of Economic Paleontologists and Mineralogists, Fifteenth Annual Research Conference, p. 139-150.

IKEDA, S., PARKER, G. AND SAWAI, K., 1981, Bend theory of river meanders: Part I, Linear development: *Journal of Fluid Mechanics*, 112, 363-377.

IMRAN, J., PARKER, G. AND KATOPODES, N., 1998, A numerical model of channel inception on submarine fans: *Journal of Geophysical Research Oceans*, 103(C1), 1219-1238.

IMRAN, J., PARKER, G. AND PIRMEZ, C., 1999, A nonlinear model of flow in meandering submarine and subaerial channels: *Journal of Fluid Mechanics*, 400, 295-331.

INMAN, D.L., NORDSTROM, C.E. AND FLICK, R.E., 1976, Currents in submarine canyons; an air-sea-land interaction: *Annual Review of Fluid Mechanics*, 8, 275-310.

LAMB, M., TONIOLO, H. AND PARKER, G., 2001, Deposition by turbidity currents in intraslope diapiric minibasins: results of 1-D experiments and numerical modeling: *Eos Trans. AGU*, 82(47).

LAMB, M.P., HICKSON, T., MARR, J.G., SHEETS, B., PAOLA, C. AND PARKER, G., 2004, Surging versus continuous turbidity currents: flow dynamics and deposits in an experimental intraslope minibasin: *Journal of Sedimentary Research*, 74(1), p. 146-155.

LIU, J.Y., AND BRYANT, W.R., 2000, Sea floor morphology and sediment paths of the northern Gulf of Mexico deepwater: Chapter 4, *Fine-Grained Turbidite Systems* (A.H. Bouma, and C.G. Stone, eds.), AAPG Memoir 72, SEPM Special Publication 68, 33-45.

MAFAFFIE, M.J., 1994, Reservoir classification for turbidite intervals at the Mars discovery, Mississippi Canyon 807, Gulf of Mexico. In: Weimer, P., Bouma, A.H., and Perkins, B.F. eds., Submarine fans and turbidite systems – sequence stratigraphy, reservoir architecture, and production characteristics: Gulf Coast Section, Society of Economic Paleontologists and Mineralogists, Fifteenth Annual Research Conference, p. 233-244.

MALINVERNO, A., RYAN, W.B.F., AUFFRET, G., AND PAUTOT, G., 1988, Sonar images of the path of recent failure events on the continental margin off Nice, France. In:

Clifton, E.H. (Ed.) Sedimentologic consequences of convulsive geologic events, *Geol. Soc. Am. Special Paper* 229, p. 59-76.

MASTBERGEN, D. R. AND VAN DEN BERG, J. H., 2003, Breaching in fine sands and the generation of sustained turbidity currents in submarine canyons: *Sedimentology*, 50(4), 625-637.

MULDER, T., AND SYVITSKI, J.P.M., 1995, Turbidity currents generated at river mouths during exceptional discharges to the world oceans: *J. Geology* 103, 285-299.

NORMARK, W. R. AND DICKSON, F. H., 1976, Man-made turbidity currents in Lake Superior: *Sedimentology*, 23, 815-831.

PANTIN, H. M., 1979, Interaction between velocity and effective density in turbidity flow: phase-plane analysis, with criteria for auto-suspension: *Marine Geology*, 46, 307-327.

PARKER, G., 1982, Conditions for the ignition of catastrophically erosive turbidity currents: *Marine Geology*, 46, 307-327.

PARKER, G., FUKUSHIMA, Y., AND PANTIN, H.M., 1986, Self-accelerating turbidity currents: *Journal of Fluid Mechanics* 171, pp. 145-181.

PARKER, G., TONIOLO, H., MARR, J., PAOLA, C., AND HICKSON, T., 2001, Modeling of Submarine Debris Flows and Turbidity Currents: Implications for Deepwater Stratigraphy: Abstracts, American Association of Petroleum Geologists, 2001 Annual Convention, June 3-6.

PARSONS, J.D. AND GARCÍA, MH., 2000, Enhanced sediment scavenging due to double-diffusive convection: *Journal of Sedimentary Research*, 70, 47-52.

PIRMEZ, C., 1994, Growth of a submarine meandering channel-levee system on Amazon Fan: *Ph.D. thesis*, Columbia University, New York, 587 p.

PIRMEZ, C., BEAUBOUEF, R.T., FRIEDMANN, S.J., AND MOHRIG, D.C., 2000, Equilibrium Profile and Baselevel in Submarine Channels: Examples from Late Pleistocene Systems and Implications for the Architecture of Deepwater Reservoirs: *GCSSEPM Foundation 20th Annual Research Conference*, Deep-Water Reservoirs of the World, Dec. 3-6, 782-805.

PRATSON, L. F. AND HAXBY, W.F, 1997, Panoramas of the seafloor: *Scientific American*, 4, 82-87.

PRATSON, L. F., IMRAN, J., PARKER, G., SYVITSKI, J. P. M. AND HUTTON, E., 2000, Debris flows versus turbidity currents: a modeling comparison of their dynamics and deposits. In: *Fine-grained turbidite systems* A. H. Bouma and C. G. Stone, eds., AAPG Memoir 72 /SEPM Special Publication 68, 57–72.

PRATSON, L.F., IMRAN, J., HUTTON, E., PARKER, G., AND SYVITSKI, J.P.M., 2001, BANG1D: A one-dimensional Lagrangian model of turbidity current mechanics: *Computers and Geosciences*, 27(6), 701-716, 2001.

PUIG, P. OGSTON, A.S., MULLENBACH, B.L., NITTROUER, C.A., AND STERNBERG, R.W., 2003, Shelf-to-canyon sediment-transport processes on the Eel continental margin (Northern California): *Marine Geology*, 193(1-2), 129-149.

SPARKS, R.S.J., BONNECAZE, R. T., HUPPERT, H. E., LISTER, J. R., HALLWORTH, M. A., MADER, H. AND PHILLIPS, J., 1993, Sediment-laden gravity currents with reversing buoyancy: *Earth and Planetary Science Letters*, 114, 243-257.

TONIOLO, H., 2002, Debris flow and turbidity current deposition in the deep sea and reservoirs: *Ph.D thesis*, University of Minnesota, 233 p.

TONIOLO, H., PARKER, G., VOLLER, V. AND BEAUBOUEF, R.T., submitted, Depositional turbidity currents in diapiric minibasins on the continental slope: experiments, numerical simulation and upscaling: *Journal of Sedimentary Research*.

TWICHELL, D.C., KENYON, N.H., PARSON, L.M., AND MCGREGOR, B.A., 1991, Depositional patterns of the Mississippi Fan surface: Evidence from GLORIA II and high-resolution seismic profiles. In: *Seismic Facies and Sedimentary Processes of Modern and Ancient Submarine Fans*, Weimer, P. and Link, M.H., eds.,Springer-Verlag, New York, NY, 349-364.

VIOLET, J., EVANS, C., SHEETS, B., PAOLA, C., PRATSON, L. AND PARKER, G., 2001, Filling of a salt-withdrawal minibasin on the continental slope by turbidity currents: Experimental Study: *Eos Trans. AGU*, 82(47).

WINKER, C.D., 1996, High-resolution seismic stratigraphy of a late Pleistocene submarine fan ponded by salt-withdrawal mini-basins on the Gulf of Mexico continental slope: *Proceedings* of the 28th annual Offsore technology conference, p. 619-628.

FIGURE CAPTIONS

Figure 1 a) View of the northern continental slope of the Gulf of Mexico showing many minibasins associated with salt withdrawal. The majority of basins are connected by turbidity current channels.

b) A detailed view of the minibasin topography of Figure 1a. Both images are courtesy of Lincoln Pratson.

Figure 2 a) Acoustic image of seafloor bathymetry in the East Breaks region, northern continental slope of the Gulf of Mexico, illustrating four minibasins and canyons in between. The channel connecting the minibasins is shown in black: the flow was from top to bottom. Basin IV has no outlet.

b) Profile of water depth from mean sea level to the bed along the Eastern Channel that connects Basins I, II, III and IV in Figure 2a. Basin IV does not have an outlet.

c) Profile of channel depth along the transect of Figure 2b, showing that the channel is deeply incised into the ridges between the basins. The images are adapted from Beauboeuf and Friedman (2000).

Figure 3 a) Photograph of a hydraulic jump in an open channel. The flow was on at the time the photograph was taken and was from left to right.

b) Sketch of supercritical open-channel flow into a deep basin, showing the hydraulic jump, the ponded zone and overflow at the downstream lip. The flow is from left to right.

Figure 4 a) Sketch of a turbidity current undergoing a hydraulic jump mediated by a sudden drop in bed slope to zero. The flow is from left to right. The turbidity current is vented

out at the downstream end by means of a submerged free overfall. The configuration corresponds to the experiments of Garcia and Parker (1989) and Garcia (1993).
b) Sketch of a turbidity current undergoing a hydraulic jump mediated by a high barrier at the downstream end of the basin. The flow is from left to right. Venting of the turbidity current can only occur if it overtops the barrier. The configuration corresponds to the experiments of the companion paper, Toniolo et al. (submitted).
c) Photograph of a horizontal settling interface of a ponded turbidity current during an experiment in the series reported by Lamb et al. (2004). The flow was on and quasi-steady at the time the photograph was taken, and was from right to left. The fluid above the glassy interface is sediment-free water, not air.

Figure 5 Illustration of a settling interface in a cylinder.

Figure 6 a) Sketch of a quasi-steady flow of a turbidity current into a deep minibasin, showing the supercritical turbidity current, the hydraulic jump and the ponded zone. Two interfaces are shown for the ponded zone, one above and one below the downstream lip. The flow is from left to right.
b) Sketch of the setup to quasi-steady flow in a downstream minibasin as the flow begins to overspill the upstream basin. At time t_1 the upstream basin has not yet overspilled; by time t_2 overspill has occurred, a critical Froude number has been established at the lip of the upstream basin, and the head of the turbidity current has progressed into the downstream basin; by time t_3 a bore has reflected off the downstream end of the downstream minibasin and is migrating upstream; and by time t_4 a quasi-steady flow has been established in the downstream minibasin.

Figure 7 a) Bathymetry of Lake Superior in the vicinity of Silver Bay, Minnesota, showing the deep trough immediately offshore. The elevations are in feet.
b) Transmissivity measurements in Lake Superior along a transect extending southeast from Silver Bay, showing a ponded turbidity current subject to seiching on July 31, 1972, near the beginning of a shutdown of the Reserve Mine due to a strike.
c) Transmissivity measurements in Lake Superior along the same transect as Figure 6b on August 2, 1972.
d) Transmissivity measurements in Lake Superior along the same transect as Figure 6b on August 8, 1972.
e) Transmissivity measurements in Lake Superior along the same transect as Figure 6b on August 19, 1972.

f) Transmissivity measurements in Lake Superior along the same transect as Figure 6b on August 24, 1972. The images are courtesy of William Normark.

Figure 8 Diagram illustrating the application of the analytical solution to the simple case of a basin with a horizontal bed, a vertical downstream barrier and no overflow. The analytical solution prevails after the hydraulic jump.

Figure 9 Diagram illustrating the actual vertical profile of suspended sediment concentration of a highly ponded turbidity current, and the approximation of the profile with a step function.

Figure 10 Diagram illustrating tendency of the pressure force to restore a tilted interface of a highly ponded turbidity current to a nearly-horizontal profile.

Figure 11 Diagram illustrating multiple settling interfaces in a muddy pond containing a discrete number of sediment sizes.

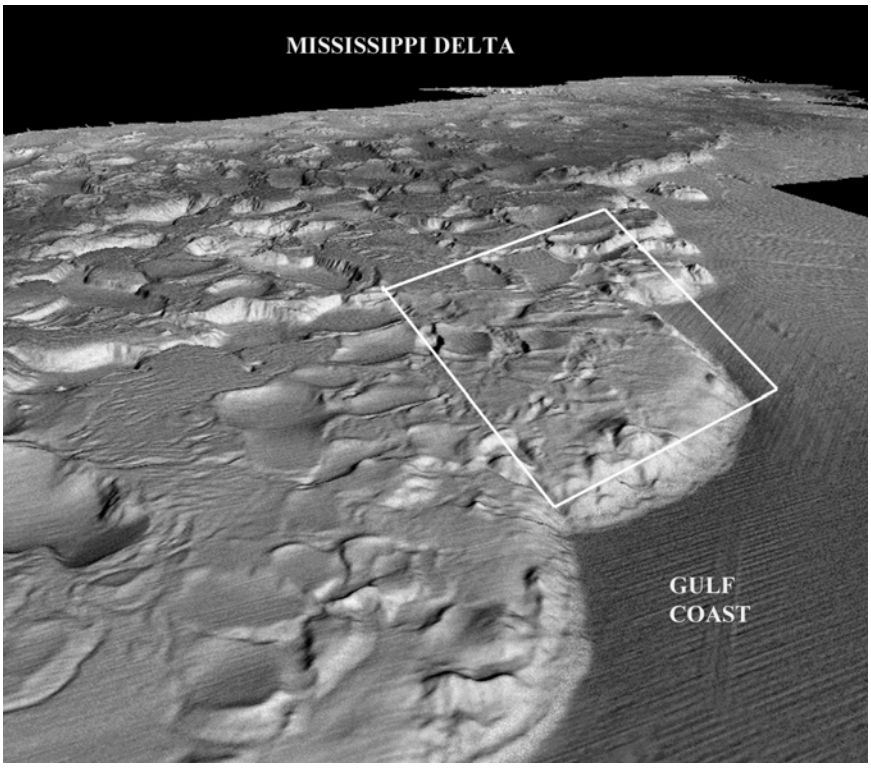

Figure 1a

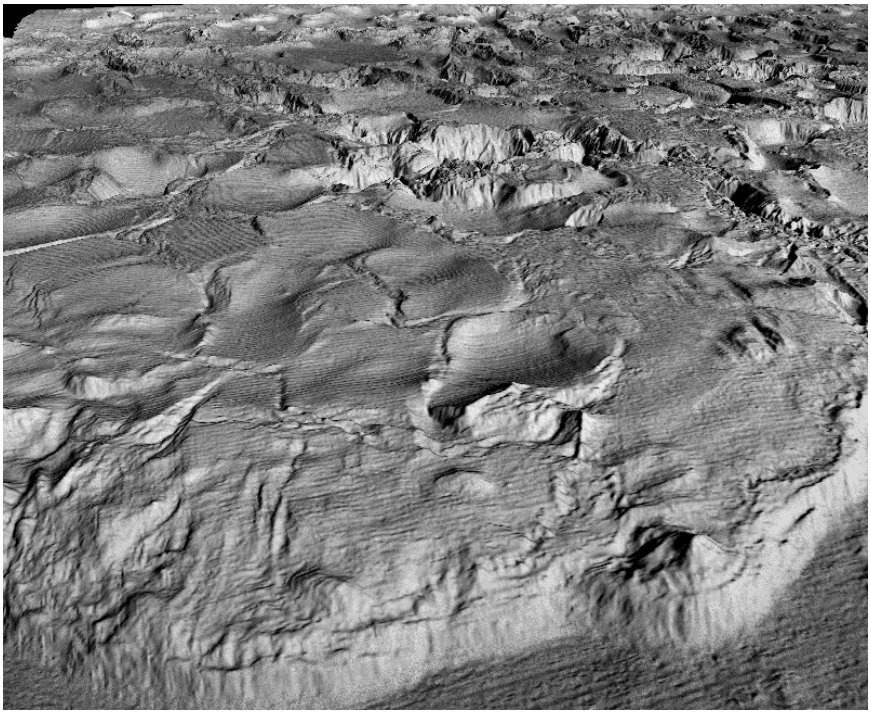

Figure 1 b

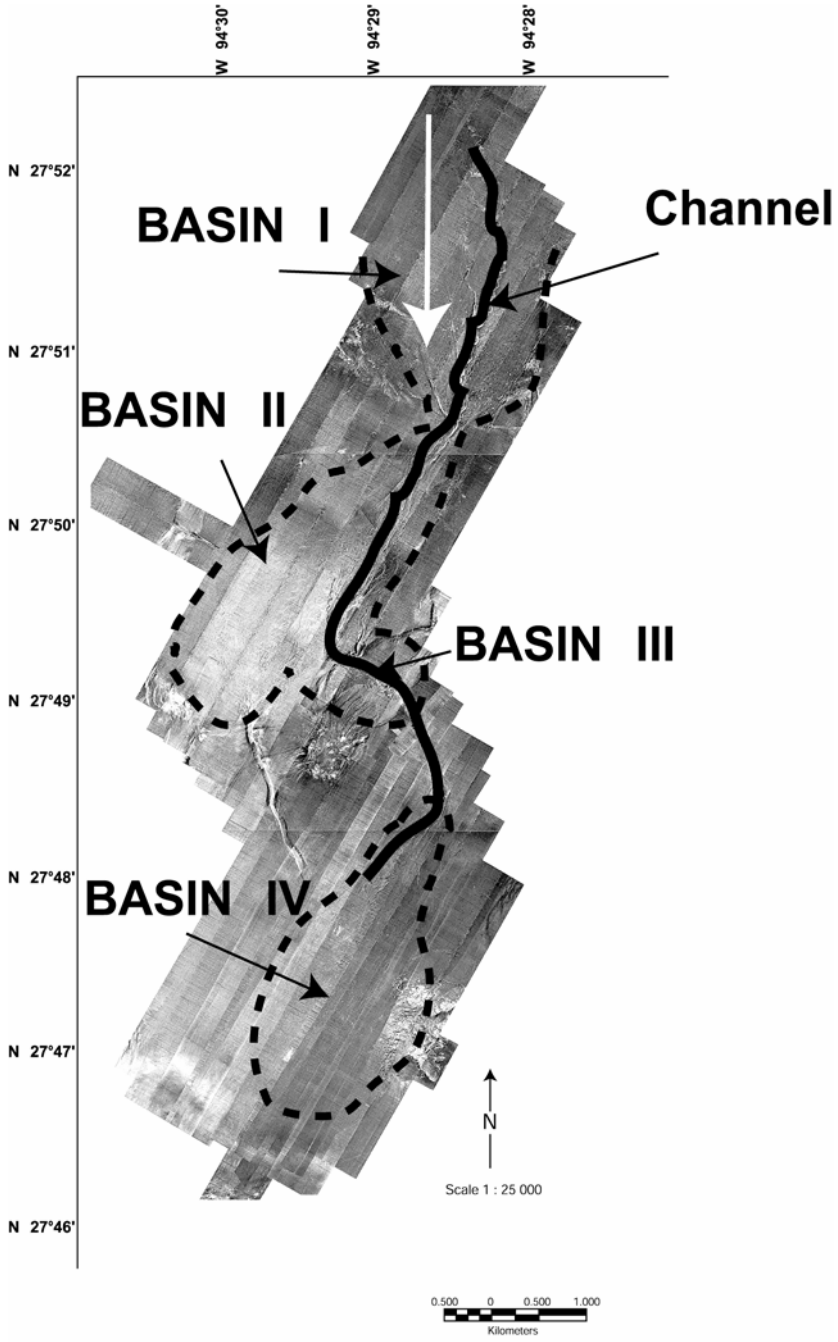
W 94°30'
W 94°29'
W 94°28'
N 27°52'
N 27°51'
N 27°50'
N 27°49'
N 27°48'
N 27°47'
N 27°46'
BASIN I
Channel
BASIN II
BASIN III
BASIN IV
N
Scale 1 : 25 000
0.500 0 0.500 1.000
Kilometers

Figure 2a

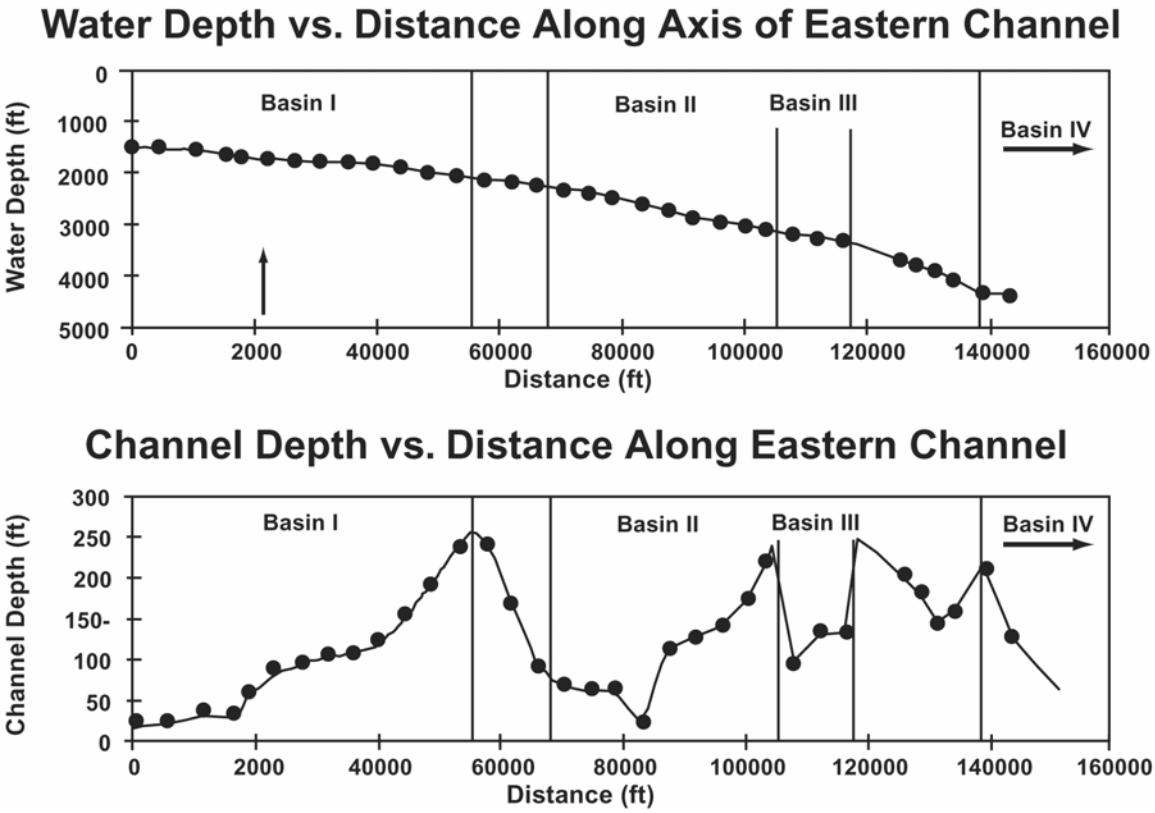

Figure 2 b and c

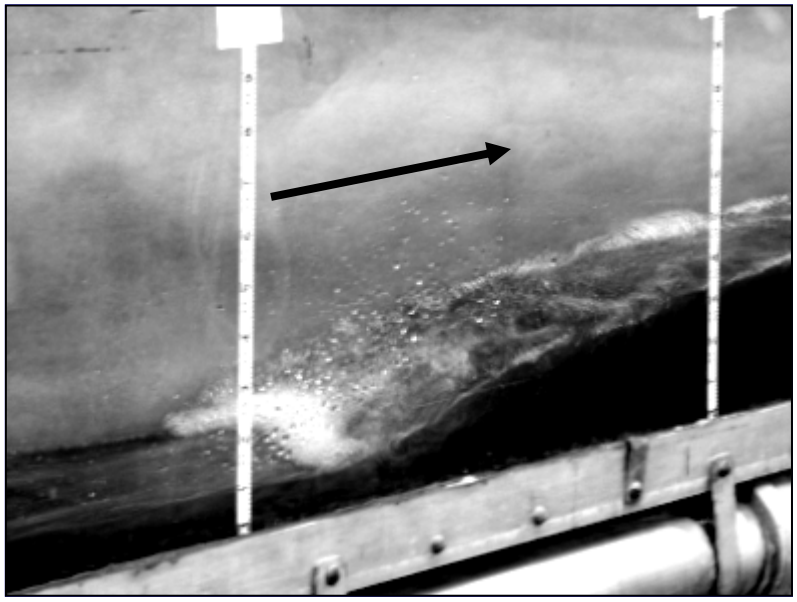

Figure 3 a

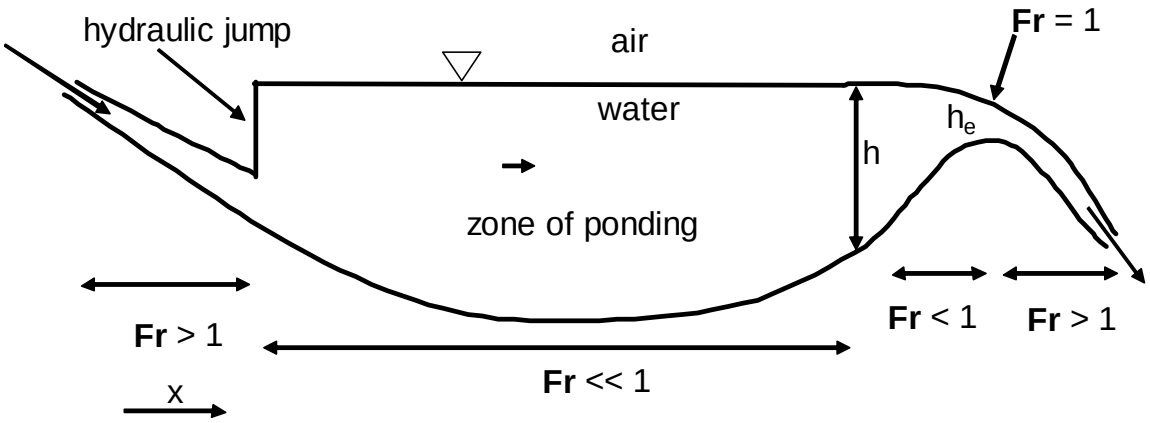

Figure 3 b

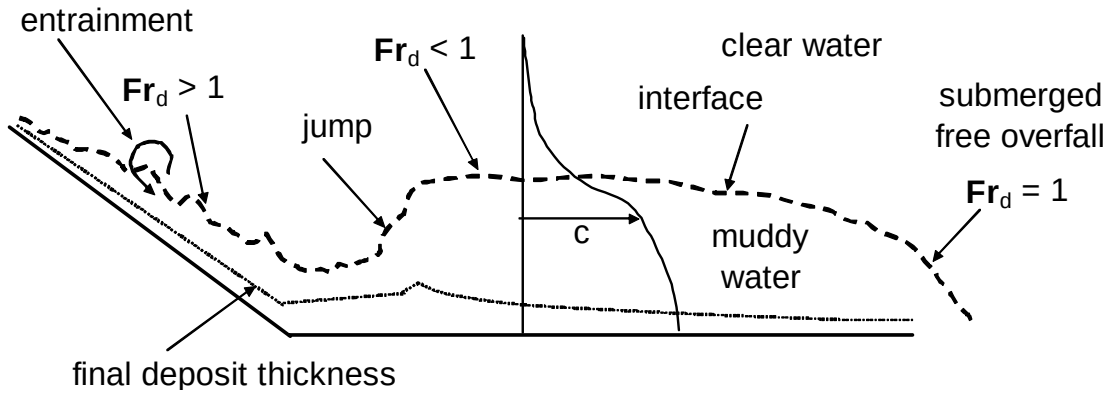

Figure 4 a

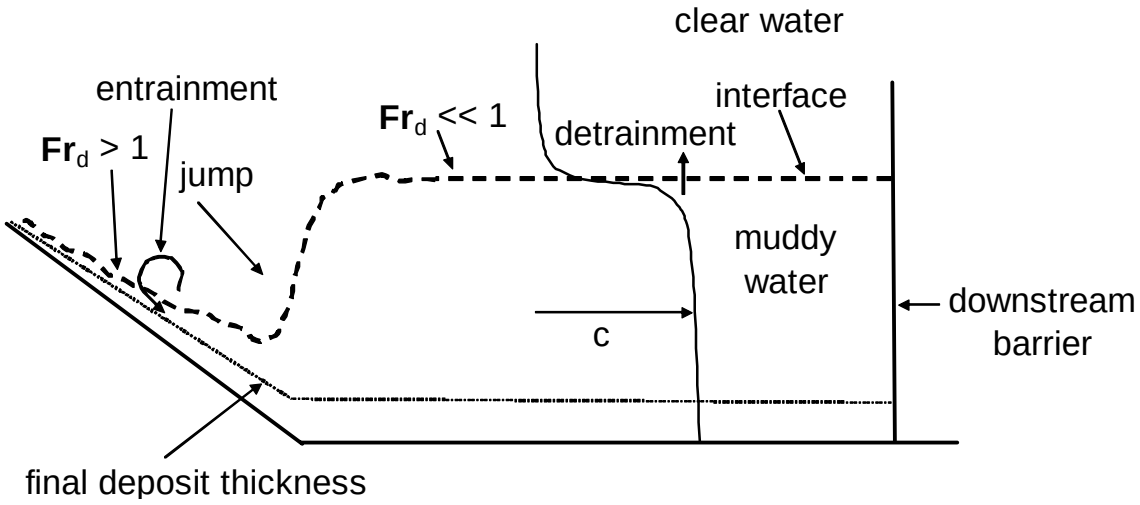

Figure 4 b

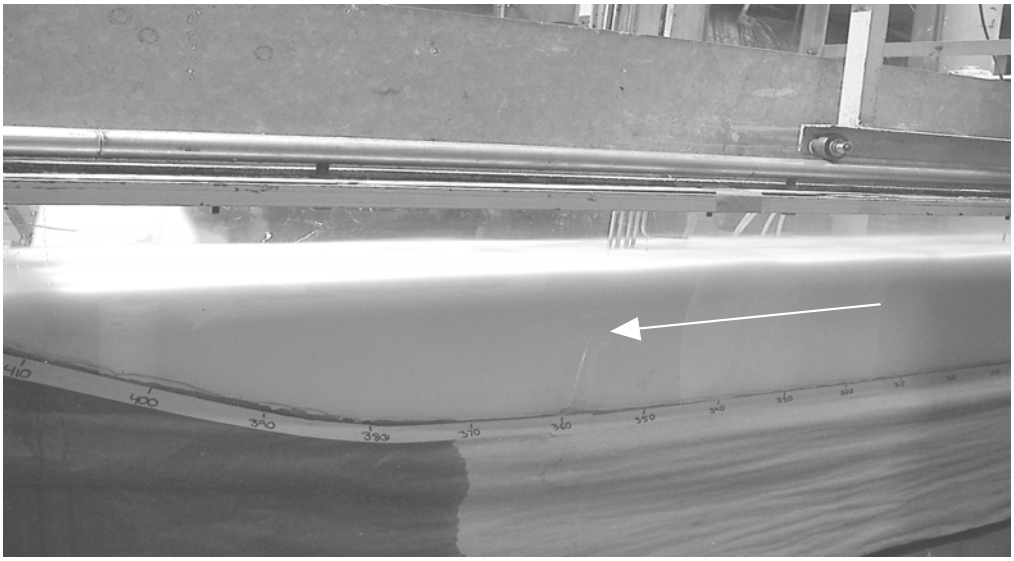

Figure 4 c

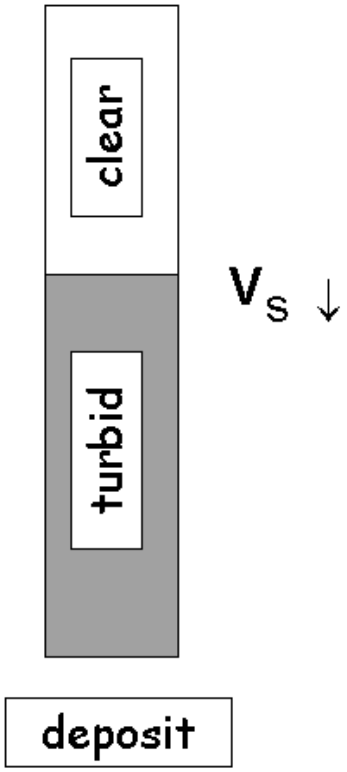

Figure 5

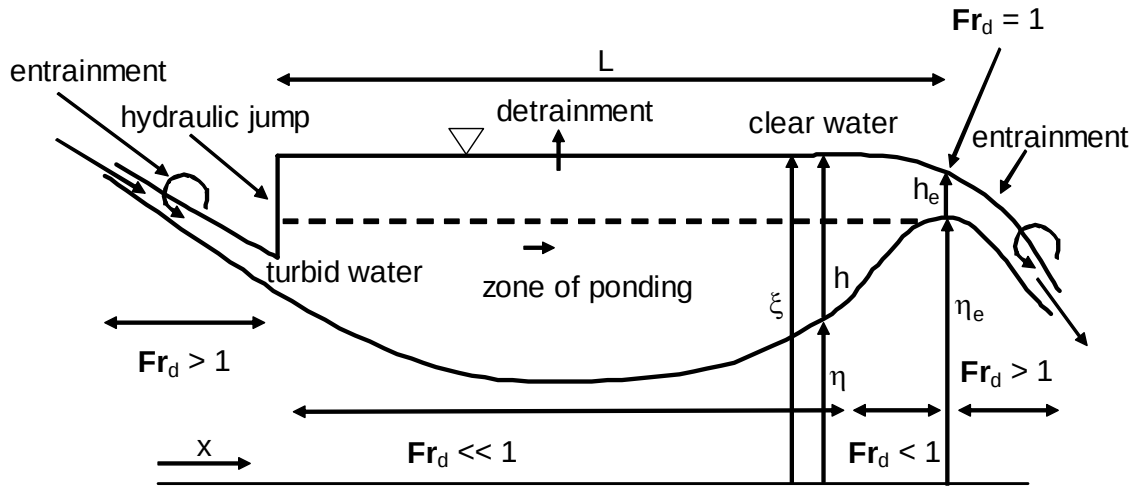

Figure 6 a

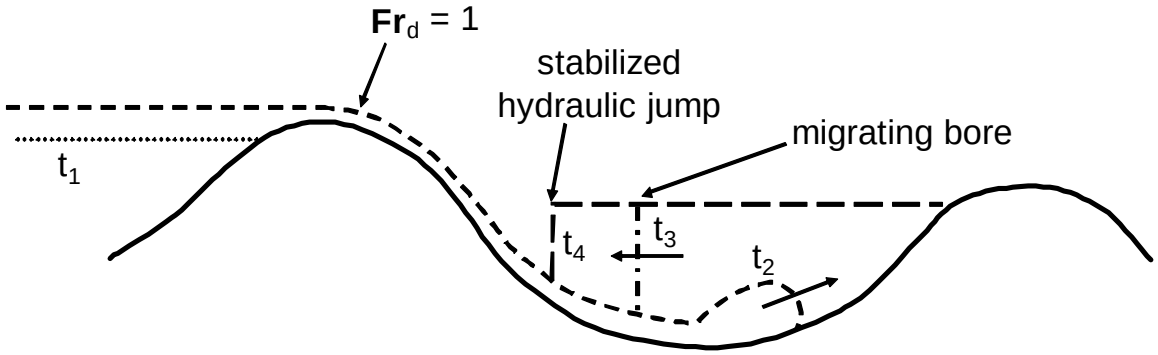

Figure 6 b

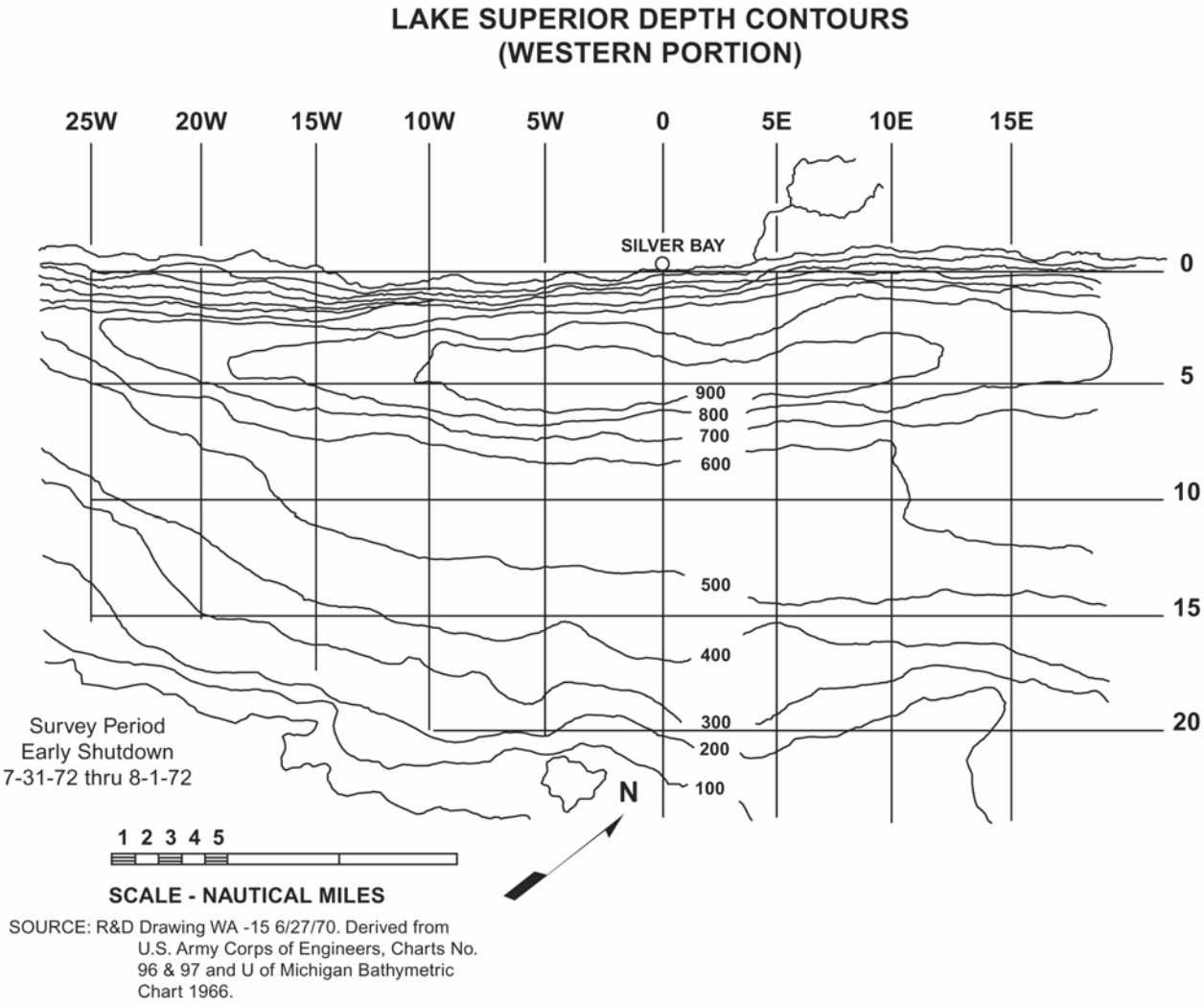
LAKE SUPERIOR DEPTH CONTOURS
(WESTERN PORTION)
25W
20W
15W
10W
5W
0
5E
10E
15E
SILVER BAY
0
5
10
15
20
900
800
700
600
500
400
300
200
100
Survey Period
Early Shutdown
7-31-72 thru 8-1-72
N
1 2 3 4 5
SCALE - NAUTICAL MILES
SOURCE: R&D Drawing WA -15 6/27/70. Derived from U.S. Army Corps of Engineers, Charts No. 96 & 97 and U of Michigan Bathymetric Chart 1966.

Figure 7 a

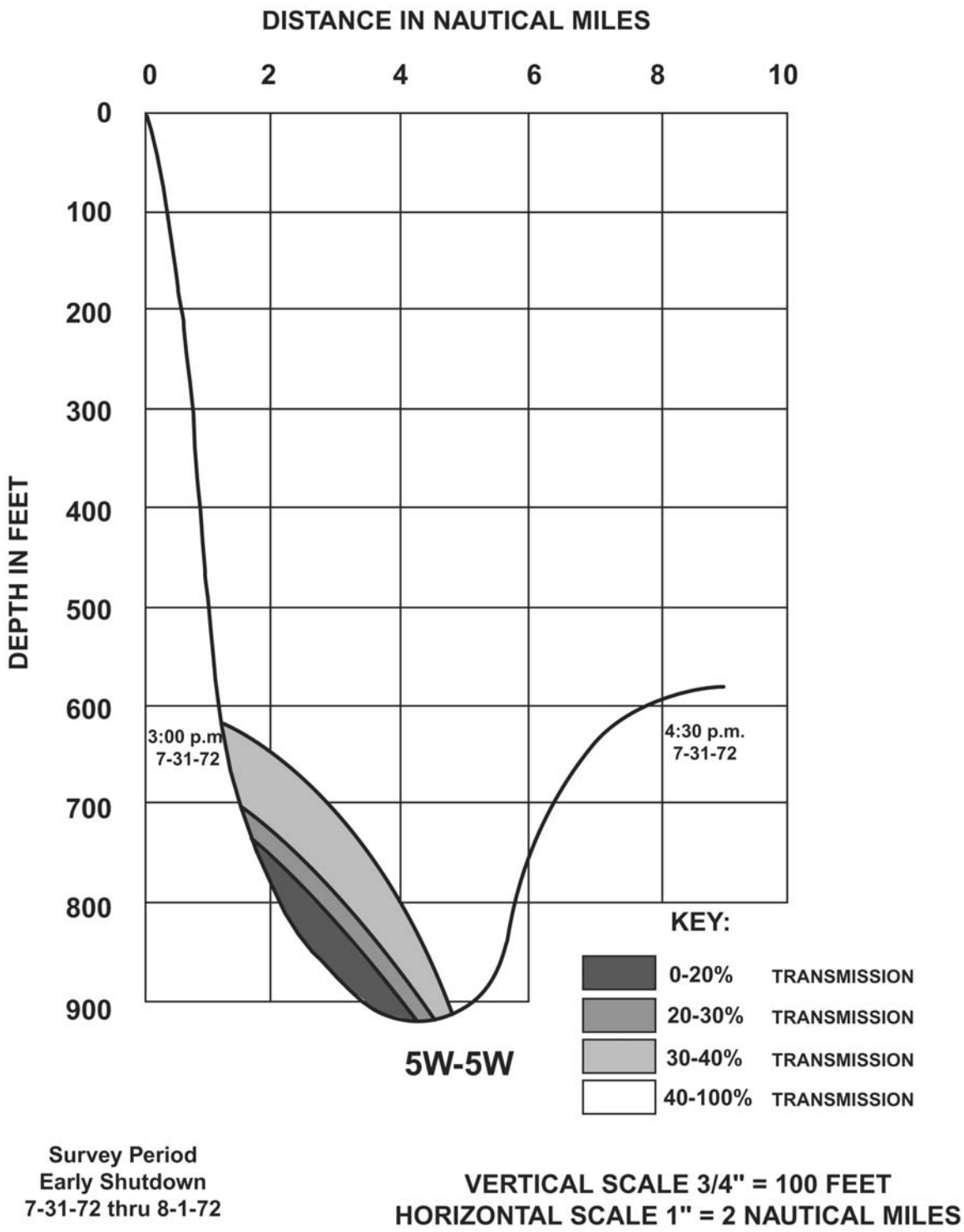
DISTANCE IN NAUTICAL MILES
0
2
4
6
8
10
DEPTH IN FEET
0
100
200
300
400
500
600
700
800
900
3:00 p.m.
7-31-72
4:30 p.m.
7-31-72
5W-5W
KEY:
0-20% TRANSMISSION
20-30% TRANSMISSION
30-40% TRANSMISSION
40-100% TRANSMISSION
Survey Period
Early Shutdown
7-31-72 thru 8-1-72
VERTICAL SCALE 3/4" = 100 FEET
HORIZONTAL SCALE 1" = 2 NAUTICAL MILES

Figure 7 b

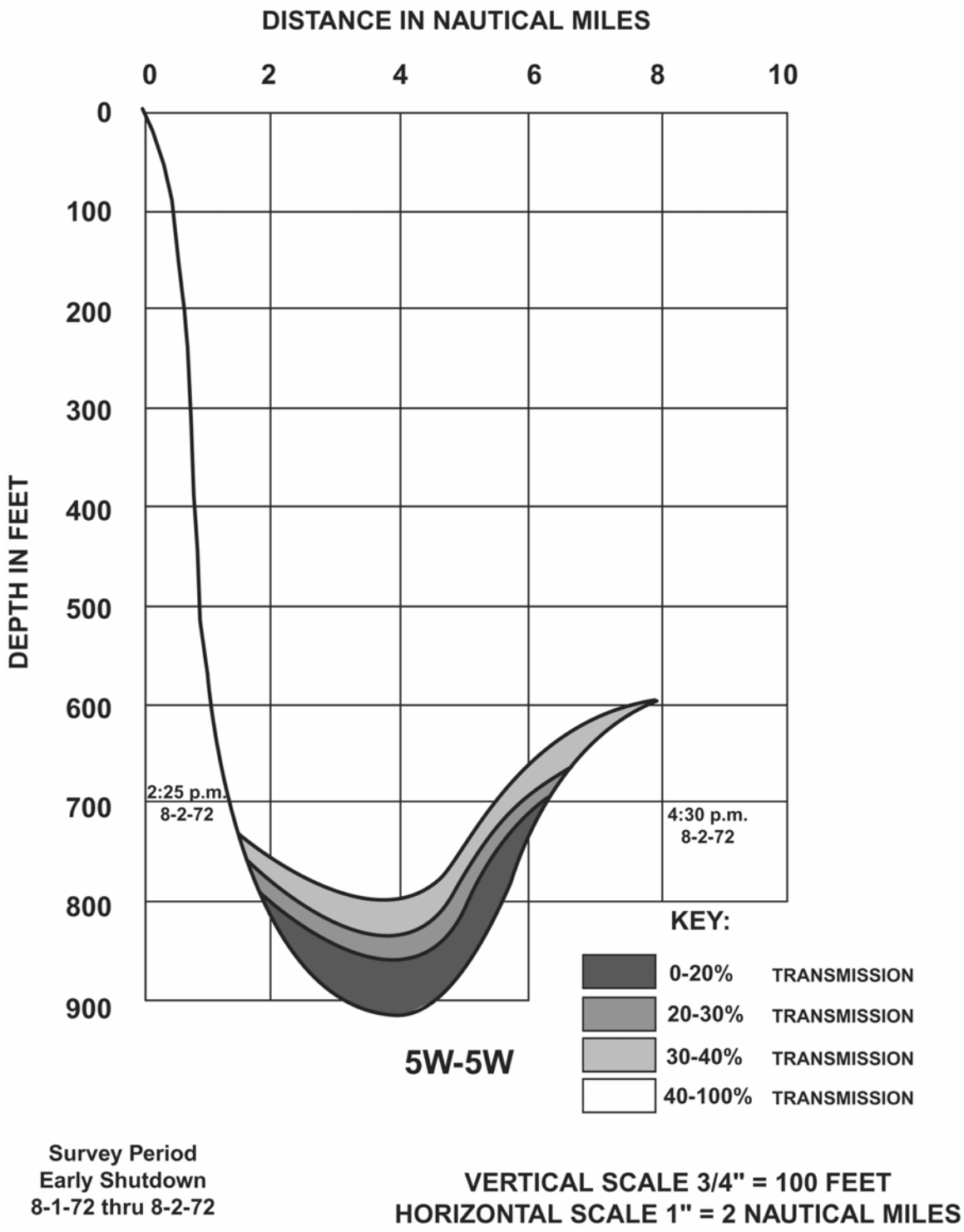
DISTANCE IN NAUTICAL MILES
0
2
4
6
8
10
DEPTH IN FEET
0
100
200
300
400
500
600
700
800
900
2:25 p.m.
8-2-72
4:30 p.m.
8-2-72
KEY:
0-20% TRANSMISSION
20-30% TRANSMISSION
30-40% TRANSMISSION
40-100% TRANSMISSION
5W-5W
Survey Period
Early Shutdown
8-1-72 thru 8-2-72
VERTICAL SCALE 3/4" = 100 FEET
HORIZONTAL SCALE 1" = 2 NAUTICAL MILES

Figure 7 c

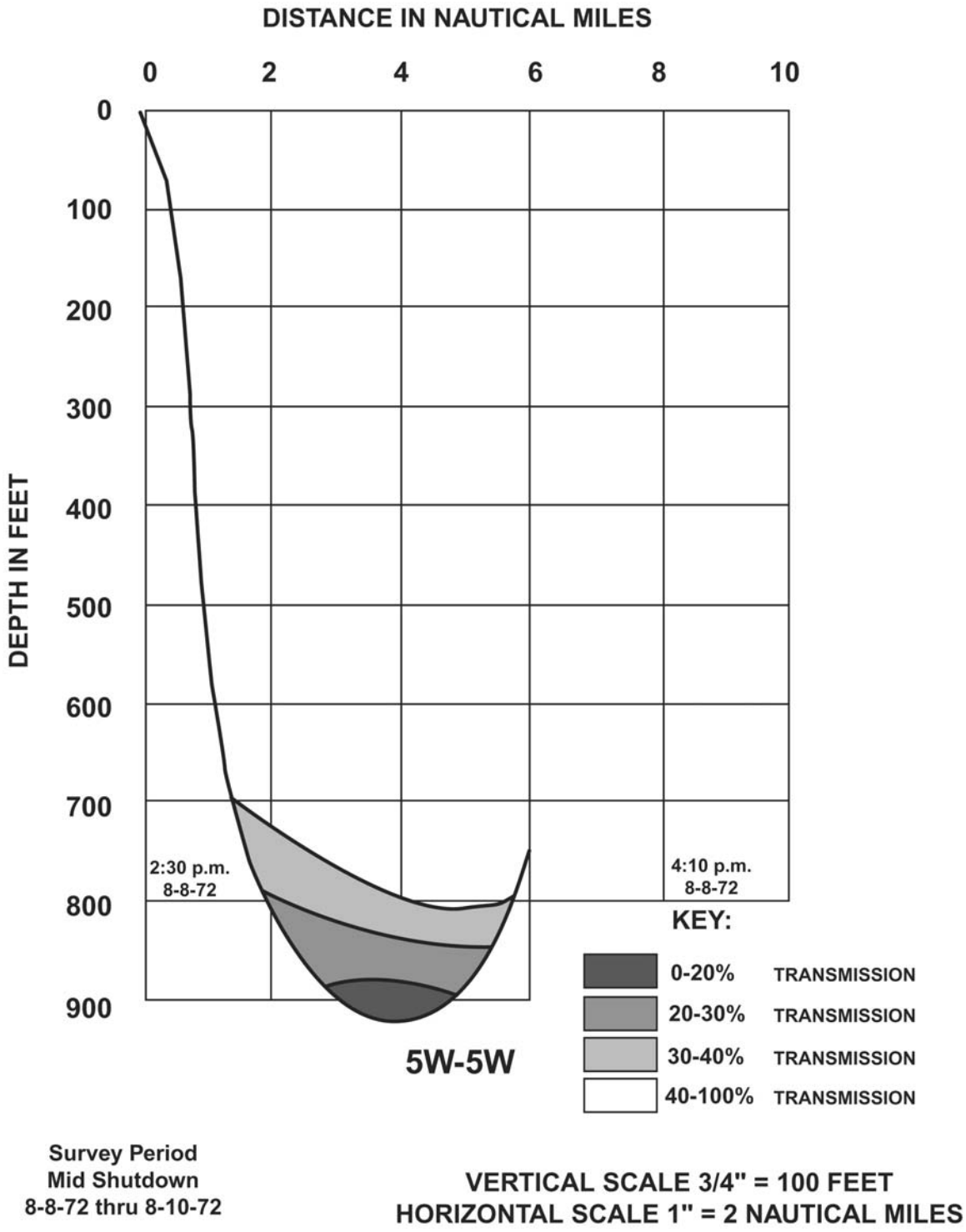
DISTANCE IN NAUTICAL MILES
0
2
4
6
8
10
DEPTH IN FEET
0
100
200
300
400
500
600
700
800
900
2:30 p.m.
8-8-72
4:10 p.m.
8-8-72
KEY:
0-20% TRANSMISSION
20-30% TRANSMISSION
30-40% TRANSMISSION
40-100% TRANSMISSION
5W-5W
Survey Period
Mid Shutdown
8-8-72 thru 8-10-72
VERTICAL SCALE 3/4" = 100 FEET
HORIZONTAL SCALE 1" = 2 NAUTICAL MILES

Figure 7 d

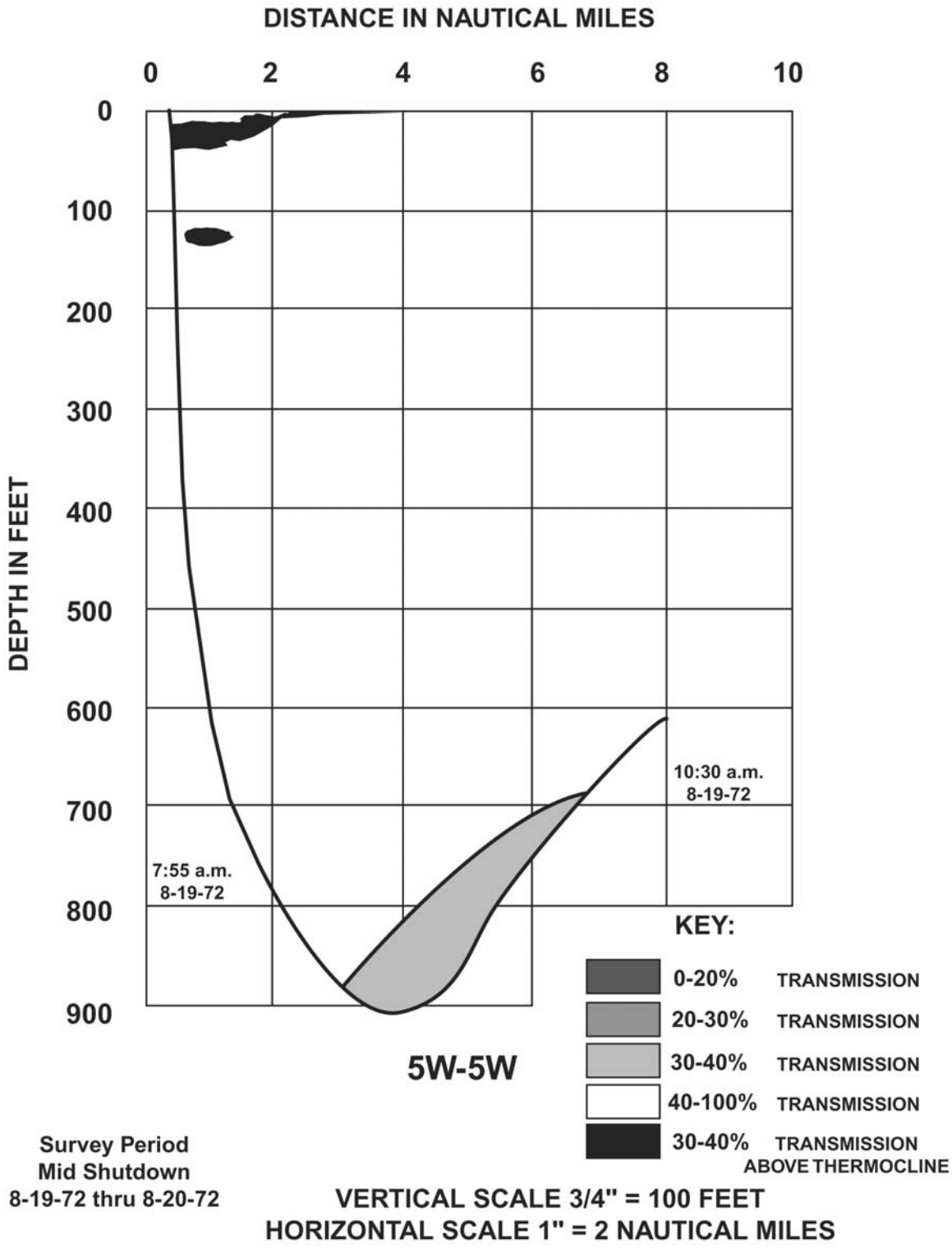
DISTANCE IN NAUTICAL MILES
0
2
4
6
8
10
DEPTH IN FEET
0
100
200
300
400
500
600
700
800
900
10:30 a.m.
8-19-72
7:55 a.m.
8-19-72
KEY:
0-20% TRANSMISSION
20-30% TRANSMISSION
30-40% TRANSMISSION
40-100% TRANSMISSION
30-40% TRANSMISSION
ABOVE THERMOCLINE
5W-5W
Survey Period
Mid Shutdown
8-19-72 thru 8-20-72
VERTICAL SCALE 3/4" = 100 FEET
HORIZONTAL SCALE 1" = 2 NAUTICAL MILES

Figure 7 e

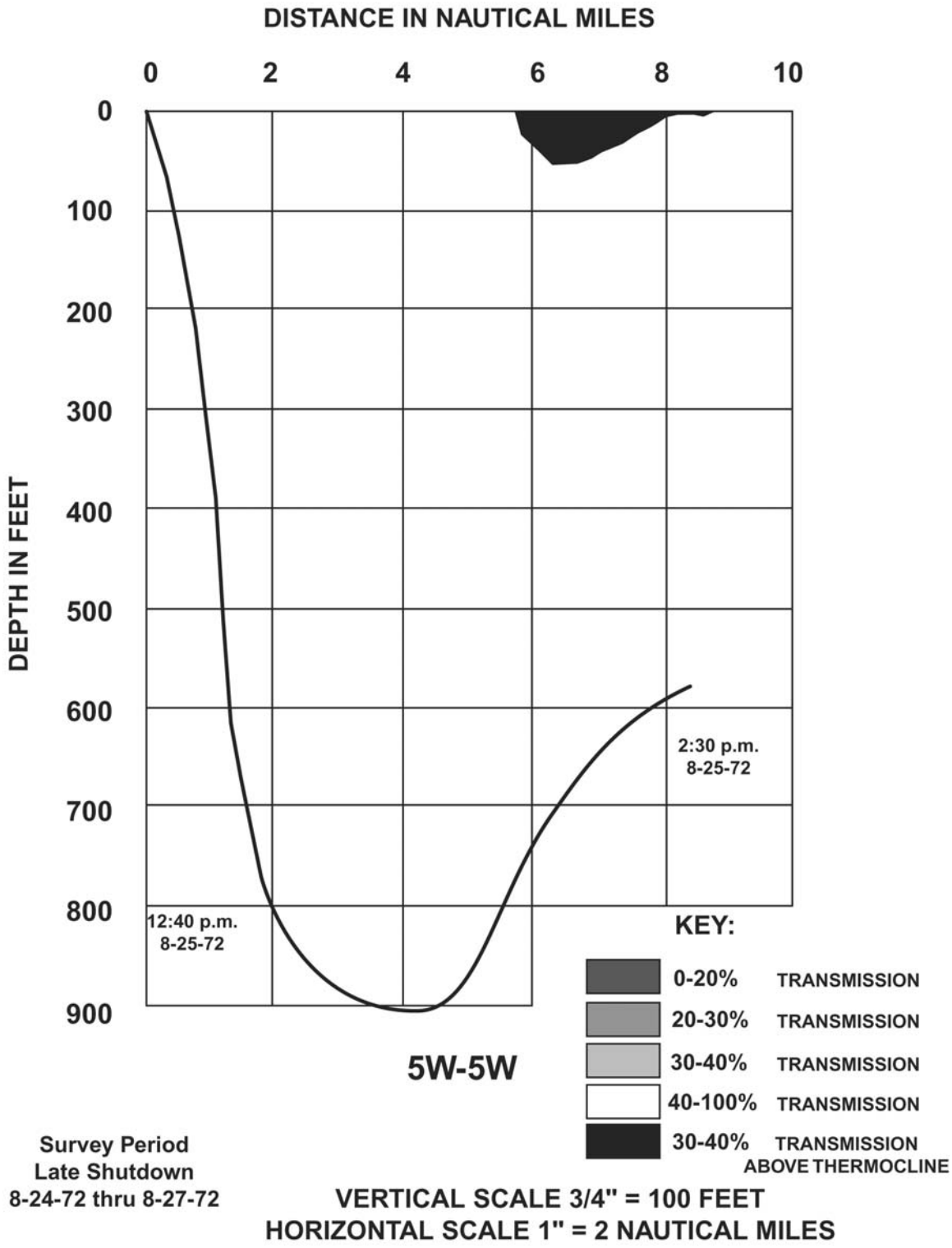
DISTANCE IN NAUTICAL MILES
0
2
4
6
8
10
DEPTH IN FEET
0
100
200
300
400
500
600
700
800
900
2:30 p.m.
8-25-72
12:40 p.m.
8-25-72
5W-5W
KEY:
0-20% TRANSMISSION
20-30% TRANSMISSION
30-40% TRANSMISSION
40-100% TRANSMISSION
30-40% TRANSMISSION
ABOVE THERMOCLINE
Survey Period
Late Shutdown
8-24-72 thru 8-27-72
VERTICAL SCALE 3/4" = 100 FEET
HORIZONTAL SCALE 1" = 2 NAUTICAL MILES

Figure 7 f

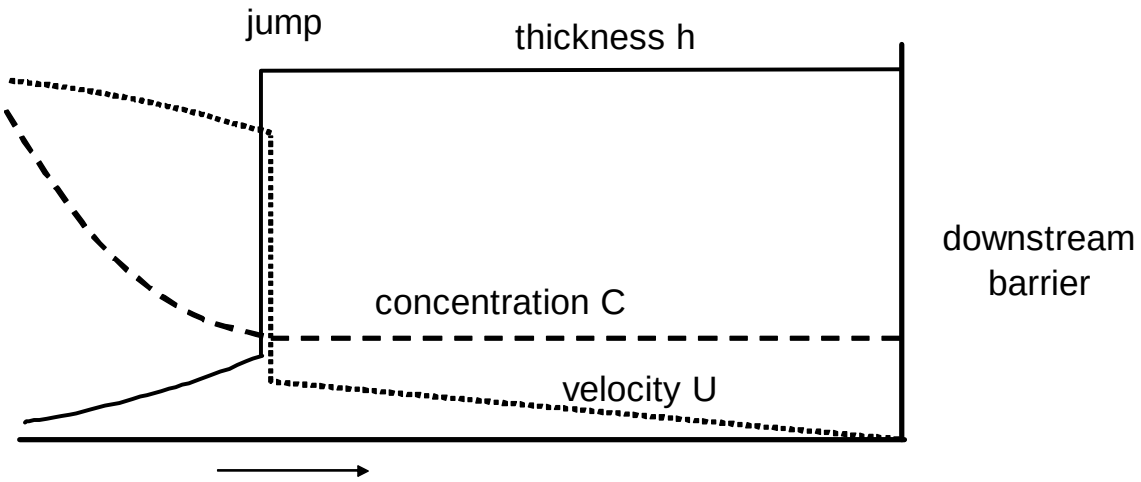

Figure 8

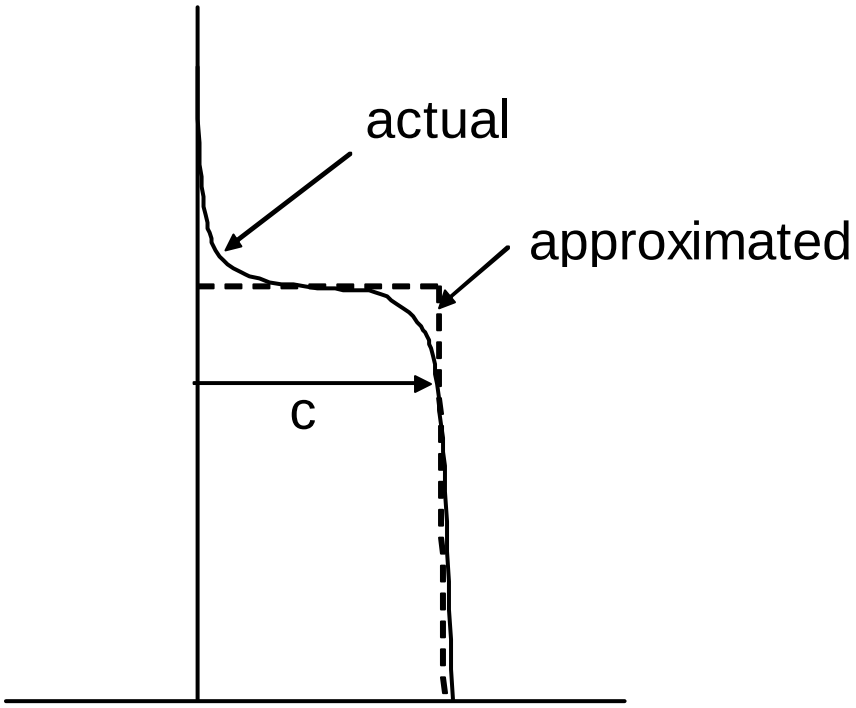

Figure 9

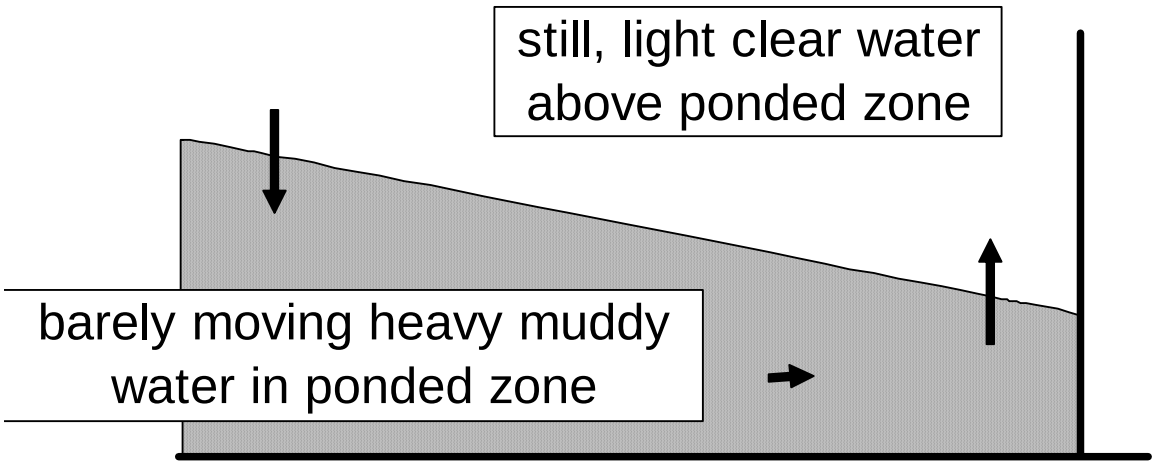

Figure 10

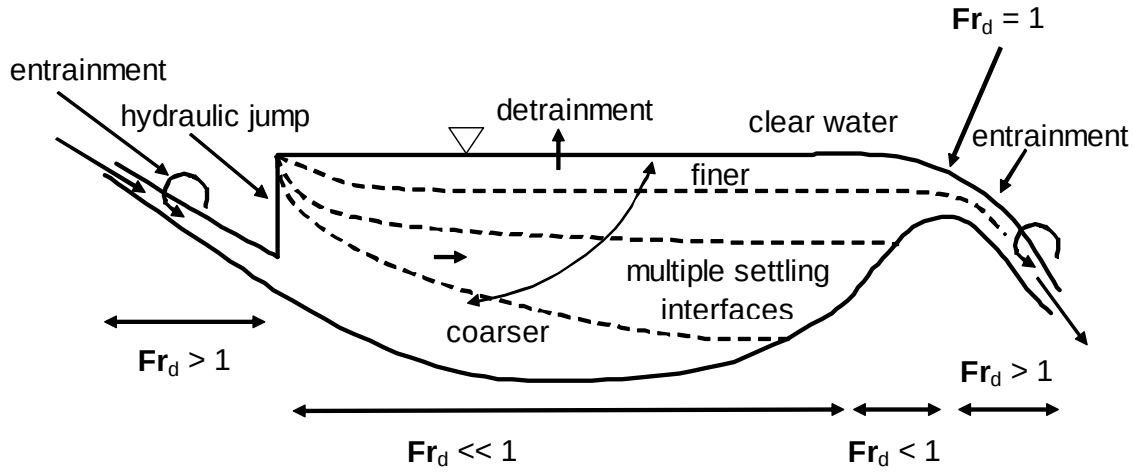

Figure 11